



UPPSALA  
UNIVERSITET



UPTEC W 21040

Examensarbete 30 hp  
Juli 2021

# Phosphorus accumulation in constructed wetlands

A study of 10 wetlands constructed on  
agricultural clay soils in Södermanland

---

Gabriella Corbee

## ABSTRACT

### Phosphorus accumulation in constructed wetlands - A study of 10 wetlands constructed on agricultural clay soils in Södermanland

*Gabriella Corbee*

Eutrophication is a major problem causing algal blooms and impaired water quality, especially regarding coastal areas and seas. It is a result of an excessive supply of nutrients such as phosphorus (P), where agriculture accounts for the largest share of the anthropogenic nutrient load. Furthermore, arable fields with clay soils have been shown to have among the highest P-losses. In this study, 10 constructed wetlands located in agricultural areas with high clay content in the topsoil were examined. The aims were to investigate how the P accumulation is related to wetland design and catchment factors and to see if there is an optimal hydraulic load (HL) and wetland size for P accumulation. The study is based on P analyses of sediment cores sampled in March 2021, calculations of catchment factors in ArcMap, water flow calculations, and statistical analyses.

Sedimentation of particles with associated P is considered to be the primary process for P retention in wetlands. Accordingly, the results showed that the P accumulation was positively correlated to particle retention. The total P accumulation varied between 8 and 96 kg ha<sup>-1</sup> yr<sup>-1</sup> and the total particle accumulation was 7-130 t ha<sup>-1</sup> yr<sup>-1</sup>. The wetland design factors, including wetland area, water depth, and length-to-width ratio (L:W), had no significant influence on the P accumulation. However, water depths greater than 1.5 m inhibited the P retention which suggested that the water depth should be limited to approximately 1 m to avoid too large particle settling distances.

The proportion of agricultural land within each catchment did not show any correlation to the P accumulation. The clay content in the topsoil was however positively correlated to both particle and P accumulation. This suggested that the sedimentation process was promoted even though the inflowing particles potentially consisted of a large proportion of clay particles, which have a low sedimentation velocity.

The erosion risk of the catchment area had no significant influence on the P accumulation, meaning that a high expected particle load did not entail an increased particle and associated P accumulation. High HL values of 450 and 850 m yr<sup>-1</sup> were shown to counteract the P retention. This corresponded to wetlands smaller than 0.1% of the catchment area. A possible turning point of HL where the P accumulation is inhibited could also be distinguished, ranging between HL 200 and 300 m yr<sup>-1</sup>. An optimal HL for increased P accumulation could not be determined due to such few observations. However, it could be concluded that an HL up to approximately 210 m yr<sup>-1</sup> had a positive influence on the particle and P accumulation and that wetlands should be larger than 0.1% of the catchment area to efficiently retain P.

**Keywords:** Phosphorus retention, sedimentation, hydraulic load

*Department of Soil and Environment, Swedish University of Agricultural Sciences (SLU), Lennart Hjelm's väg 9, SE 756 51 Uppsala, Sweden.*

## REFERAT

### Fosforackumulering i anlagda våtmarker - En studie av 10 våtmarker anlagda i jordbruksområden med hög lerhalt i Södermanland

*Gabriella Corbee*

Övergödning är ett stort problem som orsakar algblomningar och försämrade vattenkvalitet, särskilt vid kustområden och hav. Övergödningen orsakas av ett för stort utsläpp av näringsämnen såsom fosfor (P), där jordbruket står för den största antropogena näringsbelastningen. Åkermark med lerjord har dessutom visat sig ha bland den högsta utlakningen av P. I denna studie har 10 våtmarker anlagda i jordbruksområden med hög lerhalt undersökts. Syftet var att undersöka hur P-ackumuleringen är relaterad till våtmarksutformningen och abiotiska faktorer i avrinningsområdet. Projektet syftade även till att undersöka ifall det finns en optimal hydraulisk belastning (HL) för P-ackumulering. Studien baserades på P-analyser av sedimentproppar provtagna i mars 2021, beräkningar av avrinningsområdesfaktorer i ArcMap, flödesberäkningar samt statistiska analyser.

Den primära reningsprocessen för P i våtmarker är genom sedimentation av partiklar med bundet P. Följaktligen visade resultatet att P-ackumuleringen var positivt korrelerad med partikelretentionen. Den totala P-ackumuleringen varierade mellan 8 och 96 kg ha<sup>-1</sup> år<sup>-1</sup> och den totala partikelackumuleringen var 7-130 ton ha<sup>-1</sup> år<sup>-1</sup>. Våtmarksutformningen, vilket innefattade våtmarksarea, vattendjup och längd-bredförhållande (L:W), hade ingen signifikant betydelse för P-ackumuleringen. Vattendjup större än 1,5 m hämmade emellertid P-ackumuleringen vilket indikerade att vattendjupet bör begränsas till cirka 1 m för att partiklar ska hinna sedimentera.

Andelen jordbruksmark i avrinningsområdet hade ingen korrelation med P-ackumuleringen. Lerhalten i avrinningsområdet var däremot positivt korrelerad till både partikel- och P-ackumuleringen. Detta indikerade att sedimentationen främjats trots att de inflödande partiklarna potentiellt bestod av en stor andel lerpartiklar, vilka har en långsam sedimentationshastighet.

Erosionsrisken i avrinningsområdet hade ingen signifikant påverkan på P-ackumuleringen. En hög förväntad partikelbelastning resulterade därmed inte i en ökad partikel- och P-ackumulering. Höga HL-värden på 450 och 850 m år<sup>-1</sup> motverkade P-ackumuleringen, vilket motsvarade våtmarker som utgjorde mindre än 0,1 % av avrinningsområdet. En möjlig brytpunkt där HL hämmar P-ackumuleringen kunde urskiljas i intervallet HL 200-300 m år<sup>-1</sup>. På grund av för få observationer kunde inte en optimal HL för ökad P-ackumulering fastställas. Det kunde dock konstateras att en HL upp till cirka 210 m år<sup>-1</sup> hade en positiv inverkan på partikel- och P-ackumuleringen och att våtmarker bör utgöra minst 0,1 % av avrinningsområdet för att effektivt ansamla P.

**Nyckelord:** Fosforavskiljning, sedimentation, hydraulisk belastning

*Institutionen för mark och miljö, Sveriges Lantbruksuniversitet (SLU), Lennart Hjelmns väg 9, SE 756 51 Uppsala, Sverige.*

## **PREFACE**

This master thesis was written as the final step of the Master's Program in Environmental and Water Engineering at Uppsala University and the Swedish University of Agricultural Sciences (SLU). The study corresponded to 30 credits and was conducted at SLU. The supervisor was Pia Geranmayeh at the Department of Aquatic Sciences and Assessment at SLU, and the subject reviewer was Ingrid Wesström at the Department of Soil and Environment at SLU.

I would like to thank my supervisor Pia for excellent guidance and encouragement throughout the whole project. In addition, I would like to thank Ingrid Wesström for her incisive input regarding my report writing. I would also like to thank Faruk Djodjic and Stefan Hellgren at SLU for the data provided for this study.

Lastly, I would like to thank my friends and family for all the love and support throughout my education. A special thanks to Freja Lilja who stepped in and helped me with the fieldwork in this study – du är en fantastisk vän som alltid ställer upp!

Copyright © Gabriella Corbee and the Department of Soil and Environment, Swedish University of Agricultural Sciences.

UPTEC W 21040, ISSN 1401–5765

Digitally published in DiVA, 2021, through the Department of Earth Sciences, Uppsala University. (<http://www.diva-portal.org/>).

## POPULÄRVETENSKAPLIG SAMMANFATTNING

Övergödning är ett stort problem som drabbar vattendrag, sjöar, kustområden och hav. Övergödningen uppkommer när det sker ett ökat utsläpp av näringsämnen, såsom kväve (N) och fosfor (P), till vattnet. Detta kan leda till algblomningar och försämrad vattenkvalitet, där speciellt Östersjön har fått stora problem med så kallade ”döda bottenar”. Dessa har uppstått som en konsekvens av att syret tagit slut när stora mängder algblomning bryts ner på havets botten. En stor del av de näringsämnen som läcker ut och bidrar till en ökad övergödning kommer från jordbruksmark. Ett sätt att minska problemet är genom att anlägga våtmarker i jordbrukslandskapet. Våtmarker kan fånga upp näringsämnen och på så sätt rena det vatten som rinner vidare till omkringliggande sjöar och vattendrag. Den främsta processen för att fånga upp P är genom att partiklar sedimenterar, det vill säga att partiklar sjunker och lägger sig på våtmarksbotten i ett ackumulationslager. Detta eftersom P tenderar att binda till partiklar, där speciellt lerpartiklar har en stor förmåga att binda mycket P.

Det finns ett flertal faktorer som påverkar hur väl en våtmark kan fånga upp partiklar med bundet P. Våtmarkens utformning och storlek påverkar bland annat hur det inkommande vattnet sprids i våtmarken samt med vilken hastighet vattnet flödar. Till exempel tenderar ett stort längd-breddförhållande (L:W) av våtmarken att öka sedimentationen eftersom vatten med partiklar fördelas över en större yta. Beroende på hur djup våtmarken är kommer partiklar även ha olika stora avstånd att sedimentera till botten. Avrinningsområdet till våtmarken har också en påverkan på hur mycket P som kan fångas upp. Avrinningsområdet är landytan som bidrar med det vatten som rinner in i våtmarken. Därmed kan ett stort avrinningsområde i förhållande till våtmarksstorlek bidra till att mycket vatten når våtmarken. Detta kan innebära att stora mängder partiklar med bundet P transporteras till våtmarken, men samtidigt kan vattenflödet vara för stort för att partiklar ska hinna sedimentera. Markanvändning och jordtyp i avrinningsområdet spelar också roll, där till exempel jordbruksmark med en hög lerhalt har visat sig ha stor utlakning av P. Beroende på jordtyp är även marken mer eller mindre erosionsbenägen, det vill säga hur lätt jordpartiklar kan transporteras bort via vattenflöden.

I denna studie har 10 anlagda våtmarker i Södermanland undersökts, där våtmarkerna som valdes ut är anlagda i jordbruksområden med hög lerhalt. Syftet var att undersöka hur P-ackumuleringen är relaterad till våtmarksutformningen och faktorer i avrinningsområdet. Projektet syftade även till att undersöka vilken hydraulisk belastning (HL) som medför att mycket P fångas upp i våtmarkerna, där HL är vattenflödet som når våtmarken fördelat på våtmarksarean. HL är därför starkt beroende av både våtmarkens och avrinningsområdets storlek. Studien baserades på provtagning av sedimentproppar i våtmarkerna, vilket utfördes i mars 2021. En P-analys gjordes sedan av sedimentet för att kunna beräkna mängden fosfor som samlats upp samt den totala mängden partiklar som sedimenterat.

Resultatet visade att P-ackumuleringen hade ett positivt samband med partikelretentionen; desto större mängd partiklar som hade sedimenterat, desto mer P hade ackumulerat i våtmarken. Detta stämde därmed överens med teorin kring att P fångas upp i våtmarker genom att vara bundet till partiklar som sedimenterat. Den totala P-ackumuleringen visade sig

variera mellan 8 och 96 kg ha<sup>-1</sup> år<sup>-1</sup> och den totala partikelackumuleringen mellan 7 och 130 ton ha<sup>-1</sup> år<sup>-1</sup>. Detta var resultat med liknande variation som tidigare undersökta svenska våtmarker uppvisat. Våtmarksutformningen, vilket innefattade våtmarksarea, vattendjup och L:W, hade ingen signifikant betydelse för P-ackumuleringen. Vattendjup större än 1,5 m hämmade emellertid P-ackumuleringen vilket indikerade att vattendjupet bör begränsas till cirka 1 m för att partiklar ska hinna sedimentera.

Andelen jordbruksmark i avrinningsområdet hade inget samband med P-ackumuleringen. Eftersom alla våtmarker hade en stor andel jordbruksmark i avrinningsområdet är det troligt att andra faktorer hade en starkare påverkan på varför P-ackumuleringen varierar. Lerhalten i avrinningsområdet visade sig vara positivt korrelerad till både partikel- och P-ackumuleringen. Detta indikerade att sedimentationen främjats trots att de inflödande partiklarna potentiellt bestod av en stor andel lerpartiklar som har en långsam sedimentationshastighet.

Erosionsrisken i avrinningsområdet hade ingen tydlig påverkan på P-ackumuleringen. Våtmarker anlagda i mer erosionsbenägna områden, vilket kan leda till en ökad mängd inflödande partiklar, hade därmed inte en ökad partikel- och P-ackumulering. Höga HL-värden på 450 och 850 m år<sup>-1</sup> visade sig motverka P-ackumuleringen. Dessa värden motsvarade våtmarker som hade en storlek mindre än 0,1 % av avrinningsområdets storlek. En möjlig vändpunkt där HL hämmar P-ackumuleringen kunde urskiljas i intervallet HL 200-300 m år<sup>-1</sup>. På grund av få observationer av endast 10 våtmarker kunde inte en optimal HL för ökad P-ackumulering fastställas. Det kunde dock konstateras att en HL upp till cirka 210 m år<sup>-1</sup> medförde en stor partikel- och P-ackumulering och att våtmarker därför bör utgöra minst 0,1 % av avrinningsområdet för att effektivt fånga upp P.

## **ABBREVIATIONS AND DEFINITIONS**

<b>Aw:Ac</b>	The wetland area relative to the catchment area
<b>Catchment area</b>	The area of land draining into the wetland
<b>CW</b>	Constructed wetland
<b>Hydraulic efficiency</b>	A measure of how well the incoming water flow is distributed over the wetland surface area
<b>HL</b>	Hydraulic load, i.e. the inflow of water relative to the wetland area
<b>L:W</b>	Length-to-width ratio, i.e. the ratio between wetland length from inlet to outlet and the average wetland width

# TABLE OF CONTENTS

<b>ABSTRACT</b> .....	<b>I</b>
<b>REFERAT</b> .....	<b>II</b>
<b>PREFACE</b> .....	<b>III</b>
<b>POPULÄRVETENSKAPLIG SAMMANFATTNING</b> .....	<b>IV</b>
<b>ABBREVIATIONS AND DEFINITIONS</b> .....	<b>VI</b>
<b>1. INTRODUCTION</b> .....	<b>1</b>
1.1. BACKGROUND .....	1
1.2. AIM AND RESEARCH QUESTIONS .....	2
<b>2. THEORY</b> .....	<b>2</b>
2.1. NUTRIENT RETENTION PROCESSES IN WETLANDS .....	2
2.2. DESIGNS OF CONSTRUCTED WETLANDS .....	3
2.3. HYDRAULIC LOAD .....	4
2.4. SOIL PARTICLE RETENTION .....	5
2.4.1. Settling velocities of particles .....	5
2.4.2. Wetland design .....	5
2.4.3. Aggregates impact on clay particle retention .....	6
2.4.4. Wetland vegetation .....	6
<b>3. METHOD</b> .....	<b>8</b>
3.1. WETLAND SELECTION .....	8
3.1.1. Wetland criteria .....	8
3.1.2. Site description .....	8
3.1.3. Location of inlets and outlets .....	11
3.1.4. Wetland area and relative size to catchment area .....	11
3.1.5. Catchment area .....	11
3.1.6. Proportion of agricultural land .....	11
3.1.7. Length-to-width ratio .....	12
3.1.8. Soil particle size distribution within the catchment .....	12
3.1.9. Land use distribution .....	12
3.5. MODELED HYDRAULIC LOADS .....	13
3.6. EROSION RISK CLASS .....	13
3.7. MODELED PHOSPHORUS LOAD AND RETENTION .....	13
3.8. SEDIMENT SAMPLING .....	14
3.9. PHOSPHORUS ANALYSIS .....	16
3.10. TOTAL PHOSPHORUS AND PARTICLE ACCUMULATION IN SEDIMENT .....	17

3.11. STATISTICAL ANALYSIS.....	17
<b>4. RESULTS.....</b>	<b>18</b>
4.1. HYDRAULIC LOADS, EROSION RISK CLASS, AND MODELED P LOADS.....	18
4.2. SEDIMENT CHARACTERIZATION .....	19
4.3. ANNUAL SEDIMENT ACCUMULATION.....	21
4.4. TOTAL PHOSPHORUS AND PARTICLE ACCUMULATION .....	25
4.4.1. Wetland design and relative size to catchment affecting P and DW accumulation .....	27
4.4.2. Proportion of agricultural land and clay content in the catchment area affecting P and DW accumulation .....	29
4.4.3. Modeled loads and erosion risk class affecting P and DW accumulation .....	31
<b>5. DISCUSSION .....</b>	<b>38</b>
5.1. SEDIMENT ACCUMULATION IN THE WETLAND SECTIONS.....	38
5.2. THE PHOSPHORUS AND PARTICLE ACCUMULATION IN WETLAND SEDIMENT.....	40
5.2.1. Modeled P load and potential P retention.....	40
5.2.2. Particle retention and clay content in the topsoil influencing P accumulation .....	41
5.2.1. Design, relative size to catchment, and erosion risk influencing total P and DW accumulation .....	43
5.2.3. Hydraulic load and efficiency influencing total P and DW accumulation .....	44
5.3. METHOD UNCERTAINTIES .....	45
5.3.1. Sediment sampling and measurement .....	45
5.3.2. Software and statistical analysis .....	45
5.3.3. Modeled hydraulic load.....	46
<b>6. CONCLUSIONS.....</b>	<b>47</b>
<b>REFERENCES .....</b>	<b>48</b>
<b>APPENDIX .....</b>	<b>51</b>
A.1. PARTICLE SIZE DISTRIBUTION OF THE TOPSOIL .....	51
A.2. LAND USE DISTRIBUTION IN THE CATCHMENT AREA .....	52
A.3. MAPS OF WETLAND CATCHMENT AREAS AND EROSION RISK CLASSES.....	53

# 1. INTRODUCTION

## 1.1. BACKGROUND

Eutrophication is a major problem causing algal blooms and impaired water quality, especially regarding coastal areas and seas (Naturvårdsverket 2020b). It is a result of an excessive supply of nitrogen (N) and phosphorus (P), where the Baltic Sea in particular has an extensive problem. The expansion of oxygen-free zones in the Baltic Sea is now the largest that has ever occurred since its inception in 1960 (ibid.). When the algae bloom sinks to the bottom, oxygen is being consumed as the organic material decomposes. The anoxic conditions lead to an internal load of P where the iron-bound P is released from the sediment to the water (ibid.). As P is being released it contributes to more algal blooms, which can aggravate the lack of oxygen.

The Swedish Environmental Protection Agency's annual follow-up of Sweden's national environmental objectives in 2020 shows that the long-term trend indicates a decrease in total nutrient emissions to the sub-basins of the Baltic Sea (HELCOM 2019, 2020; Naturvårdsverket 2020b). However, the nutrient input during the six years period from 2012-2017 shows an increased supply of N and P from Swedish areas to several sea basins (ibid.). The nutrient supply that reaches our surrounding oceans consists of both an anthropogenic load and a background load. The background load is naturally occurring independently of human activity. Regarding the anthropogenic load of P and N, agriculture accounts for the largest share in the south of Sweden (Naturvårdsverket 2020b). Moreover, arable fields with clay soils have shown to have among the highest P-losses (Johannesson et al. 2015)

Losses of P from arable land can be transported in both particle-bound and dissolved forms (Ulén 2005). Clay particles have a large specific surface area, making it possible for P to adsorb to the surface (ibid.). Hence, clay particles can adsorb more P compared to coarser particles. By constructing wetlands, diffuse sources of nutrients and erosion material from agricultural land can be alleviated (Braskerud 2003). Constructed wetlands (CWs) can therefore be seen as a final buffer to reduce various types of pollution before reaching the recipients (Braskerud 2001b). Hence, the retention of clay particles in wetlands is of major concern to reduce the leaching of different substances, such as P (ibid.).

In an ongoing research project at the Swedish University of Agricultural Sciences, forty wetlands in clay areas around Mälardalen are investigated regarding factors such as phosphorus and carbon accumulation, and particle size distribution in wetland sediment. The project is funded by the Swedish Agency for Marine and Water Management (Havs- och vattenmyndigheten) and is titled *Reduced internal load and increased return of nutrients to agricultural land through optimal design and placement of wetlands (Minskad internbelastning och ökad återförsel av näring till jordbruksmark genom optimal utformning och placering av våtmarker)*. In this study, ten wetlands will be selected for inclusion in the research project, where they will be sampled and evaluated concerning P accumulation in wetland sediment.

## **1.2. AIM AND RESEARCH QUESTIONS**

This thesis aims to evaluate the P accumulation in wetland sediment. This will be performed by relating the P accumulation to the hydraulic load (HL), wetland size, and the proportion of agricultural land and clay content in the soil in the catchment area. Furthermore, the goal is to be able to conclude what influences the P accumulation in wetlands and whether there is an optimized wetland size for P accumulation. The research questions of the study are the following:

- I. How is the P accumulation in sediment affected by the design of the wetland (length-width ratio, size, and depth)?
- II. How is the P accumulation in sediment affected by HL and the proportion of agricultural land, clay content in the soil, and erosion risk class in the catchment area?
- III. What is the optimal HL for P accumulation in wetlands?

## **2. THEORY**

### **2.1. NUTRIENT RETENTION PROCESSES IN WETLANDS**

There are three main processes regarding nutrient retention in wetlands; denitrification, nutrient uptake of plants and algae, and sedimentation (Jordbruksverket 2004). N is retained through all three processes, where denitrification is the most important procedure. P can also be built into the biomass of plants and algae, and be physically sedimented by particles (*ibid.*). Moreover, P can be retained in the sediment by chemical bonds (Blomqvist & Rydin 2009).

Denitrification is a process where nitrate is converted to nitrogen and a small proportion of nitrous oxide. The conversion is performed by denitrification bacteria which are found on the biofilm of the macrophytes, i.e. aquatic plants, and in the wetland sediment (Jordbruksverket 2004). The formed nitrogen gas is then released into the atmosphere after being dissolved in the water, which causes N to permanently be removed from the wetland (*ibid.*).

N and P can be built up in the biomass of the plants and algae in the wetland (Jordbruksverket 2004). Whether the removal of nutrients is lasting due to plant uptake depends on the life cycle of the plants. Almost all nutrients are returned to the water when plant parts are decomposed (*ibid.*). However, if the total biomass increases or if the biomass is harvested and removed from the wetland, the nutrient removal is enduring. Moreover, P can be retained due to bacterial uptake, where the assimilated P is released by the bacteria as organic compounds (*ibid.*). The sedimentation of dead bacteria can also be of importance for the separation of P in wetlands (*ibid.*).

When water slows down as it enters the wetland, it allows particles in the water to settle to the bottom of the wetland. This sedimentation process is primarily important for the retention of inorganic particle-bound P since organic forms of both N and P tend to dissolve in the water (Jordbruksverket 2004). When sedimented organic material decomposes, both N and P are released, which can be returned to the water by diffusion (*ibid.*). Furthermore, the effect of sedimentation on nutrient retention is also affected by the resuspension of sediment (*ibid.*). As water currents, waves or animals whirl up the sediment, the material can either settle again or be carried with the water flow out of the wetland (*ibid.*). Sedimentation of particulate-P is

considered to be the process that has the greatest significance for the P-retention in wetlands (Jordbruksverket 2004; Johannesson et al. 2015).

Processes such as chemical precipitation and complex formation with metal oxides can also retain P to the sediment (Blomqvist & Rydin 2009). Chemical precipitates can be formed as P reacts with calcium (Ca) at high pH values, or with iron (Fe) and aluminum (Al) compounds at low pH values (Ulén 2005). In particular, it is common for P to bind to Fe-hydroxide complexes in the sediment (ibid.). If anoxic conditions occur or there are changes in pH, P can be released into the water. When the oxygen content at the sediment reaches zero, the binding that retains P to Fe in a complex formation ceases (ibid.). Similarly, chemical precipitates can be dissolved as the pH changes (ibid.). Hence, the processes regarding P-retention are not permanent but depend on how much P is stored in the wetland sediments.

## 2.2. DESIGNS OF CONSTRUCTED WETLANDS

CWs can be divided into three categories depending on how the wetland is supplied with water, which is illustrated in Figure 1 (Hassby et al. 2015). Some CWs receive the entire flow from a watercourse, which often occurs as the wetland is constructed by a widening of the waterway (Figure 1: A) (ibid.). The wetland can also receive water through a culvert or drainage pipe, where water exit the wetland back to the culvert or a watercourse (Figure 1: B) (ibid.). The third type is a bypass wetland, which is constructed next to a watercourse where the in- and outlets of the wetland are connected to the waterway (Figure 1: C) (ibid.). This type of CW only receives parts of the water flow and is often constructed to avoid interference in the watercourse (ibid.). Such reasons can be due to fish migration or to preserve surrounding arable land (Jordbruksverket 2004).

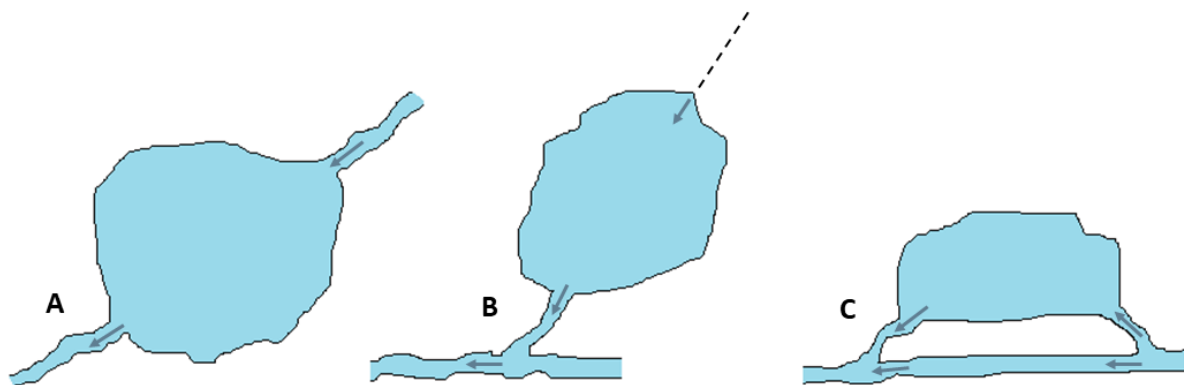


Figure 1. Different types of wetlands where A receives the entire flow from a watercourse, B receives water from a drainage pipe or culvert (marked as a dashed line), and C is a bypass wetland constructed next to a watercourse and receives only parts of the water flow from the stream. In this figure, the water exits B back to a watercourse. The arrows indicate the direction of the water flow. Illustration: Gabriella Corbee.

Examples of constructed wetlands are ponds, shallow lakes, and other water bodies which are covered with water either partly or all year round (Hassby et al. 2015). Depending on the main function of the wetland, the design usually looks different. The wetlands that have previously been constructed in Sweden have mainly been focused on N retention and the increase of biological diversity (Jordbruksverket 2010). They are generally designed as

shallow ponds with large surface areas and with a varying amount of vegetation (ibid.). In 2010, subsidies were introduced to encourage the construction of wetlands that retain P, so-called P-wetlands (ibid.). P-wetlands are designed to promote the sedimentation process and generally consist of a sedimentation basin at the inlet (depth of 1 m) (Braskerud 2001a; Jordbruksverket 2004, 2010). The following section often consists of a wetland filter, which is a shallow area with emergent plants (depth between 0.3 and 0.5 m) (Braskerud 2001a, 2003).

### 2.3. HYDRAULIC LOAD

The amount of water that reaches the wetland per time unit is referred to as the HL (Jordbruksverket 2004). The HL is highly determined based on the area of the catchment ( $A_C$ ) and how large the CW area ( $A_W$ ) is in relation to the catchment ( $A_W:A_C$ ) since this regulates the runoff volume entering the CW per day (Johannesson et al. 2015). The correlation between HL and  $A_W:A_C$  is commonly found to be negative (Kynkäänniemi 2014). Hence, the smaller the CW is in relation to its catchment, meaning a lower  $A_W:A_C$ , the higher HL is expected.

The larger the catchment is, the more nutrients can be transported to the wetland and increase the nutrient load (Jordbruksverket 2004). This applies provided that the concentration of nutrients is high in the incoming water (ibid.). The HL also affects the residence time for the water in the CW, which is reduced with a high HL (ibid.). As a result, the residence time in the wetland might become too short for particles to have time to settle.

To estimate the streamflow at an ungauged catchment, the drainage area ratio method can be applied where a known stream gauge is used as a reference (Archfield & Vogel 2010). The method is based on the following equation:

$$Qu_t = \frac{Au}{Ag} \cdot Qg_t \quad (1)$$

where  $Qu_t$  is the streamflow [ $m^3 s^{-1}$ ] at the ungauged catchment, while  $Qg_t$  is the streamflow at the reference stream gauge, both on day  $t$ .  $Au$  and  $Ag$  correspond to the drainage areas [ $m^2$ ] of the ungauged catchment and the reference stream gauge, respectively. However, Equation (1) shows that the streamflows per unit area for both catchments are equal for any given time  $t$  (Archfield & Vogel 2010). Accordingly, the amount of water that reaches a CW can be derived by knowing the annual runoff in the sub-catchment of the river basin in which the CW and its catchment are located (Equation (2)).

$$Q_{CW} = \frac{A_C}{A_B} \cdot Q_B \quad (2)$$

where  $Q_{CW}$  is the streamflow [ $m^3 s^{-1}$ ] at the CW catchment,  $A_C$  is the area [ $m^2$ ] of the CW catchment,  $A_B$  is the area of the river basin's catchment, and  $Q_B$  is the runoff in the reference stream gauge. By knowing the inflow of water and CW area, with the assumption that the runoff is the same throughout the larger catchment, the annual HL [ $m yr^{-1}$ ] can be calculated as follows:

$$HL = \frac{Q_{cw} \cdot 3600 \cdot 24 \cdot 365}{A_w} \quad (3)$$

where  $Q_{cw}$  is converted to annual flow [ $\text{m}^3 \text{yr}^{-1}$ ] and  $A_w$  is the wetland area [ $\text{m}^2$ ].

## 2.4. SOIL PARTICLE RETENTION

It is presumed that a significant part of the P that is transported from agricultural land with fine-textured soils is attached to particles (Johannesson et al. 2015). Accordingly, the most important process for P retention in wetlands is likely by sedimentation (ibid.). Several factors influence the sedimentation rates in wetlands; particle size and shape, together with the water velocity and depth of the wetland (ibid.). As a result, the design of the wetland is important regarding the sedimentation rate (ibid.).

### 2.4.1. Settling velocities of particles

Stoke's law can be used to predict the settling velocity of a small spherical particle as it sinks through a liquid column due to gravitational influence (Britannica 2016). It is expressed as the following:

$$v = \frac{2(\rho_p - \rho_l)gr^2}{9\eta} \quad (4)$$

where  $v$  is the settling velocity [ $\text{cm s}^{-1}$ ],  $\rho_p$  is the particle density [ $\text{g cm}^{-3}$ ],  $\rho_l$  is the density of the liquid [ $\text{g cm}^{-3}$ ],  $g$  is the gravitational constant [ $\text{cm s}^{-2}$ ],  $r$  is the radius of the sphere [ $\text{cm}$ ], and  $\eta$  is the viscosity of the surrounding liquid [ $\text{g cm}^{-1} \text{s}^{-1}$ ] (Braskerud 2003; Britannica 2016). As an example, using Stoke's law, a coarse clay particle with a 2  $\mu\text{m}$  diameter and density of 2.65  $\text{g cm}^{-3}$  would need 88 hours for settling in a 1-meter water column at temperatures of 15  $^\circ\text{C}$  (Braskerud 2003). However, the prediction of settling velocities using Stoke's law is based on several assumptions (Kroetsch & Wang 2008). First, the particles are spherical although most silicate clay particles are platy (ibid.). Second, the water temperature is constant throughout the sedimentation process, and third, the soil particles settling in a cylinder are not influenced by surrounding particles or the cylinder wall (ibid.). In reality, there can be processes occurring which influence the retention of particles that are complex and still not fully understood (Braskerud 2003).

### 2.4.2. Wetland design

The residence time in a wetland needs to be relatively long for the sedimentation of clay particles to be promoted (Johannesson et al. 2015). Accordingly, the HL needs to be small (ibid.). The wetland design also influences the water velocity, where elongated shapes increase the flow velocity as a result of a narrow cross-section (Persson et al. 1999). A higher velocity will therefore be obtained in a wetland with a long and narrow shape, meaning a high length-to-width ratio (L:W), compared to a wetland of the same area that is shorter and wider. A high L:W will however give a better hydraulic efficiency compared to a wetland with a low ratio, meaning that the water is distributed to a large extent over the entire water surface area (Wörman & Kronnäs 2005; Kynkäänniemi 2014). Wetlands with high L:W ratios tend to

accumulate more P, presumably explained by the increased hydraulic efficiency and water flow path which increases the residence time (Aronsson et al. 2019).

Depending on the flow conditions in the wetland, particle retention is also affected by the water depth (Braskerud 2003). For laminar flows, the trap efficiency would be the best in a shallow pond with a short vertical settling distance (ibid.). However, deeper wetland sections tend to promote sediment accumulation more than shallower open water areas since shallow areas are more exposed to sediment disturbances such as wind (Fennessy et al. 1994). The trap efficiency under turbulent conditions can be described by Equation (5) (Braskerud 2003; Sveistrup et al. 2008):

$$E = 100(1 - \exp(-wAQ^{-1})) \quad (5)$$

where  $E$  is the relative retention of particles [%],  $w$  is the sedimentation velocity [ $\text{m s}^{-1}$ ],  $A$  is the surface area [ $\text{m}^2$ ], and  $Q$  is the discharge from the wetland [ $\text{m}^3 \text{s}^{-1}$ ]. According to (5), a wetland with a small surface area and high HL [ $QA^{-1}$ ] would have a low trap efficiency since the retention of particles increases with surface area and decreases with discharge (Sveistrup et al. 2008). Hence, the trap efficiency decreases as the HL increases.

#### **2.4.3. Aggregates impact on clay particle retention**

When a group of primary soil particles coheres to each other more strongly than to other surrounding particles, they form a soil aggregate (Nimmo 2013). The formation occurs as a result of processes in the soil where attractive and disruptive forces are acting on the soil particles. This causes a greater cohesion among some particles than others (ibid.). Flocs, however, which often are used as a synonym to aggregates, are formed in the watercourse (Sveistrup et al. 2008).

Aggregated clay particles have been shown to outweigh the negative effect of an increased HL since the aggregates have a higher sedimentation velocity than single clay particles (Braskerud 2003). Hence, Stoke's law (Equation (4)) is not suitable for predicting the settling velocity of particles that tend to form aggregates and should be restricted to only indicate the relation between aggregate density, diameter, and sedimentation velocity (ibid.). Moreover, aggregates can be eroded during transport to the wetland (Sveistrup et al. 2008). Wetlands should be constructed as close as possible to the arable fields to reduce the risk of decomposition of aggregates during transport. This can potentially improve the retention performance of the wetland due to the higher sedimentation velocity of aggregates (ibid.).

#### **2.4.4. Wetland vegetation**

Vegetation in wetlands has also been shown to influence the sedimentation process (Braskerud 2001b). Vegetation can reduce both water turbulence and water velocity, which allows for increased sedimentation of particles (ibid.). The macrophytes can also provide filtering mechanisms. For instance, particles can flow into the leaves and stems and stick to the biofilm on the plants (ibid.). This filtration effect might however be negligible due to the water velocities that commonly occur in CWs (ibid.). Moreover, vegetation in wetlands can affect the formation of aggregates through flocculation (ibid.). Particle collision may increase as water passes the vegetation since vortices are formed downstream of the stems and leaves

(*ibid.*). In effect of this small-scale turbulence, flocculation is stimulated. The floc formation can also be stimulated due to the sticky organic matter which is produced by the biofilm covering the plant (*ibid.*). Wetland vegetation can also prevent the resuspension of wetland sediment (*ibid.*).

The vegetation's effect on sedimentation patterns varies, and studies have also shown negative effects of macrophytes. Dense vegetation in wetlands can block water movement, resulting in the forming of channels where sediment is moved mainly through open water areas (Fennessy et al. 1994). At the same time, vegetation can reduce short circuit water flows during high flows when the capacity of the preferential flow channels is low (Braskerud 2001b). As a result, the water passing through the wetland uses more of the wetland width which increases the hydraulic efficiency (*ibid.*).

For CWs with high HL (400 to 1200 m yr<sup>-1</sup>) and short residence time, increased vegetation has been shown not to influence the clay particle retention since the flocculation may be limited under those circumstances (Braskerud 2001b). The effect of vegetation on sediment retention can also reach a limit where the retention is more influenced by other factors, such as HL and sediment load (Braskerud 2001b). This has been observed as the vegetation cover exceeds 50% (*ibid.*).

### **3. METHOD**

#### **3.1. WETLAND SELECTION**

##### **3.1.1. Wetland criteria**

The CWs included in this study were selected based on the following criteria:

- i. The CW must have a high expected nutrient load, corresponding to a large proportion of agricultural land in the catchment area. This criterion was set to at least 50% agricultural land within the catchment, including both pasture and arable land.
- ii. The CW should preferably be limited to one in-and outlet, respectively.
- iii. The in-and outlet should be located in such a way that the incoming water passes through the whole CW area, i.e. located at the “short ends” of the wetland.
- iv. The shape should be rather long and narrow since a high L:W ratio results in high hydraulic efficiency, meaning that the inflow of water is distributed to a large extent over the CW surface area (Jordbruksverket 2004).
- v. If the CW is connected to a watercourse, it must receive the entire flow. This excludes bypass wetlands from being selected since parts of the water flow pass without entering the CW, which makes estimations of the HL inaccurate.

##### **3.1.2. Site description**

Eight wetlands were selected based on the criteria. Due to difficulties finding suitable wetlands to include in this study, two of the CWs (Hel and Kla) had two inlets each. In addition, two previously studied wetlands (Kynkäänniemi 2014; Geranmayeh et al. 2018; Ferguson 2019) with high nutrient loads and that match the above-mentioned criteria were included in this study. Available estimations performed by Ferguson (2019) were used for these two wetlands (Nyb and Okn S), which included CW areas, catchment areas, and L:W ratios. Figure 2 displays the geographical location and design of the selected CWs. Three of the CWs are P-wetlands, divided into a sedimentation basin and a shallow section with vegetation, while the other CWs are ponds. In Figure 2, the CWs characterized as P-wetlands are marked in green and the ponds in blue.

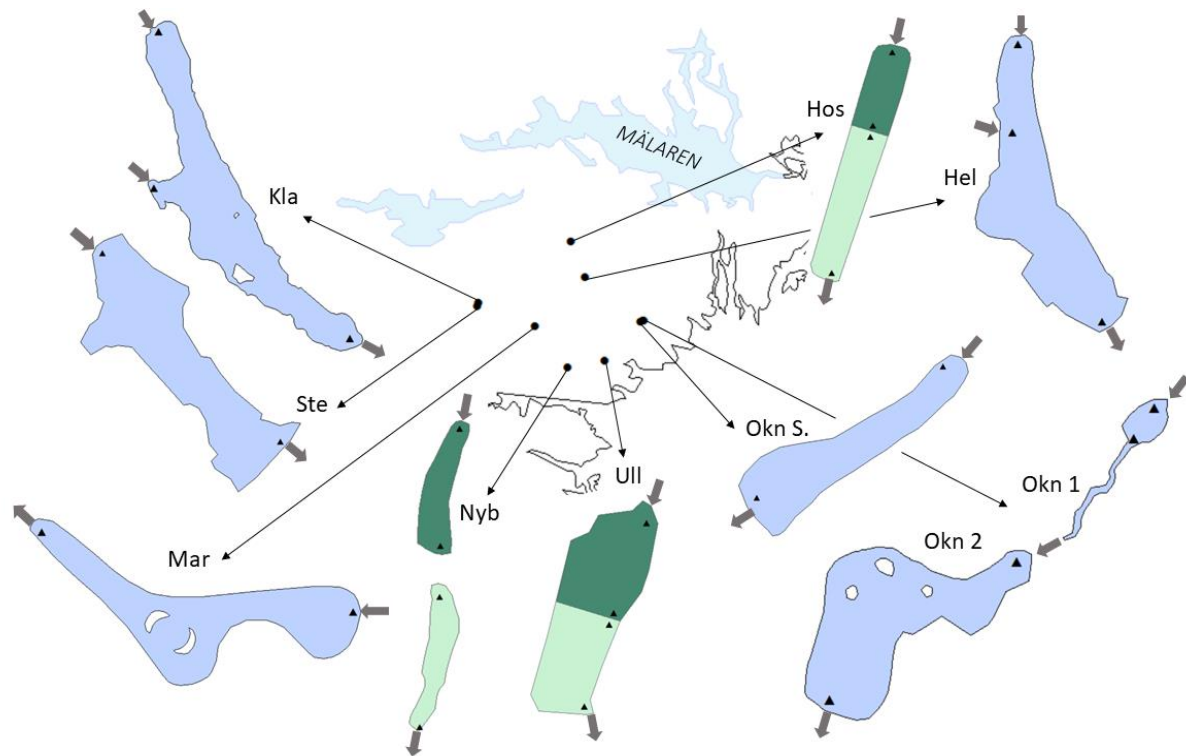


Figure 2. The geographical location and design of the selected CWs, all situated in Södermanland County. The black dots mark the location and the thin arrows point to an enlargement of the CWs. The CWs' inlets and outlets are marked as arrows and sediment sampling points as black triangles. Nyb is constructed with an embankment between the wetland sections, where the basins are connected through a drainage pipe. Okn 2 is located directly downstream of Okn 1, with an open ditch connecting the two wetlands. The sedimentation basin of the P-wetlands (Hos, Ull, and Nyb) is dark green, the shallow section is light green. Figures are not to scale. Illustration: Gabriella Corbee.

An overview of the selected CWs is presented in Table 1. The CWs are located in agricultural areas where the land cover categories that dominate most catchments are arable land, pasture, and forest (Appendix A.2.). The share of arable land and pasture within the catchments varies between 41% and 66%. The CWs vary in shape and size, with L:W ratios from 3 to 12, and areas between 0.02 ha and 6.3 ha (average area of 1.4 ha). There is a large spread in relative size between the wetland area and the associated catchment area; from 0.02% to 6.7%. Thus, two very small CWs (Okn 1 and Hos) have a large corresponding catchment area in relation to the CW area, accounting for < 0.1% of the catchment. The small CWs (Okn 2, Ull, Okn S, and Nyb) have areas less than 0.5% of the catchment area. Hel, Kla, Ste, and Mar are considered to be large CWs, which make up 3-7% of the catchment area. Maps of the CWs and their catchment areas are displayed in Appendix A.3.

Table 1. Overview of the studied CWs, year of construction, CW type, wetland type (P-wetland or pond), the estimated area of wetland water surface ( $A_w$ ), estimated catchment area ( $A_c$ ), the ratio between CW area and catchment area ( $A_w:A_c$ ), the proportion of agricultural land within the catchment (registered agricultural land in 2018 from the Swedish Board of Agriculture), and length-width ratio (L:W) of the CWs.

CW	Year	Type	$A_w$ [ha]	$A_c$ [ha]	$A_w:A_c$ [%]	Agr. land [%]	L:W
Okn <sup>a</sup>			0.79	199	0.40	52	9
Okn 1	2010	Pond	0.08	194	0.04	52	11
Okn 2	2002	Pond	0.71	5/199 <sup>b</sup>	0.35 <sup>c</sup>	52 <sup>c</sup>	4
Hos	2017	P-wetland	0.02	115	0.02	65	6
Nyb	2011	P-wetland	0.09	79 <sup>d</sup>	0.11	41	12 <sup>d</sup>
Okn S	2013	Pond	0.06	45 <sup>d</sup>	0.14	62	6 <sup>d</sup>
Ull	2010	P-wetland	0.20	127	0.16	51	3
Mar	2012	Pond	1.4	47	2.9	66	7
Kla	1998	Pond	6.3	129	4.9	53	9
Hel	2012	Pond	3.9	58	6.7	54	6
Ste	2001	Pond	1.4	20	7.1	53	4

a. The CW consist of two connected wetlands constructed in different years.

b. The total catchment area including Okn 1's catchment since Okn 2 receives the inflow of water from Okn 1.

c. Calculation based on the total catchment area (199 ha).

d. Based on estimations by Ferguson (2019).

The particle size distribution in the topsoil of the catchment is similar for the CWs, where silt is the soil fraction with the largest share (Figure 3). The silt fraction varies between 42% and 49%, where Okn S has the lowest share and Mar the largest. The sand fraction range between 16% (Hel) and 28% (Kla). The CW with the largest share of clay in the catchment is Okn S with 37%, followed by Hel and Nyb, both with 36%. The smallest proportion of clay is found in the catchment area of Kla (27%). It should be noted that Okn 2's catchment studied separately (not including the contributing catchment of Okn 1) is presented in Figure 3.

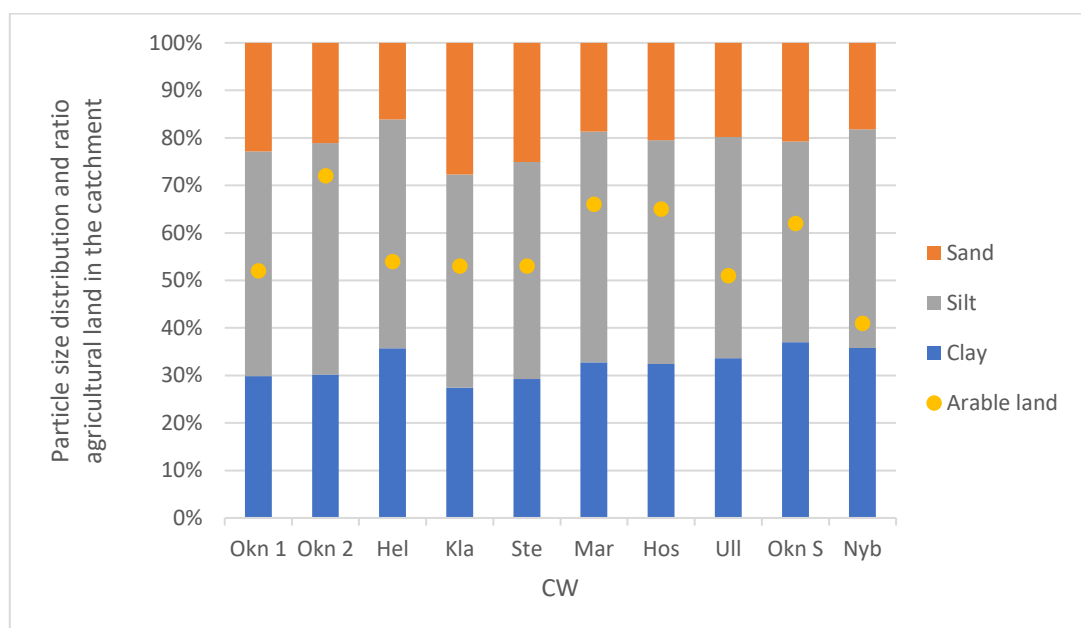


Figure 3. The particle size distribution in the topsoil of agricultural areas within CW catchments. The share of arable land within the catchment, including pasture, is indicated by a yellow circle.

### **3.1.3. Location of inlets and outlets**

The wetlands were located by reviewing available data presented as shapefiles (polygons) of CWs and their estimated catchment area (Djordjic 2021), using the cartography software ArcMap. Shapefiles of CWs around Mälardalen (without estimated catchments) and the Swedish Meteorological and Hydrological Institute (SMHI) water web's wetland database were also researched. The in- and outlets of the CWs were examined using maps such as Google Maps, Eniro, and the topographic sitemap of the Swedish Mapping, Cadastral, and Land Registration Authority (Lantmäteriet, LM). The flow direction of surrounding waterways and ditches were used as indicators of the in- and outlet location. In some cases, the county administration board or landowners were contacted due to difficulties to determine the location from map images. Kla, Mar, Okn S, and Hel are provided with water through drainage pipes (applies for one of the inlets to Hel), while the other CWs have open ditches as inlet types.

### **3.1.4. Wetland area and relative size to catchment area**

The selected CWs with available shapefiles of CW area were based on land areas registered as wetland areas and did not represent the current size of the CW water surfaces. Consequently, new polygons representing the water surface were created for all CWs using ArcMap. The areas were based on orthophotos (aerial photographs) obtained from LM. The previously studied CWs, Nyb and Okn S, with areas estimated by Ferguson (2019) were also slightly adjusted to better match the water surface seen on orthophotos. Moreover, the ratio between CW area and catchment area ( $A_W:A_C$ ) was computed by dividing CW areas by their corresponding catchment area.

### **3.1.5. Catchment area**

Since data presented as shapefiles of estimated catchment areas were available for most CWs, it was only for the Ull wetland that the catchment needed to be computed. The catchment area was computed using available flow accumulation and flow direction files (Hellgren 2021) of watersheds within which the CW and its catchment were located.

The files were processed in ArcMap by converting the raster from floating points to integers by using the *Int* tool. Thereafter, a point polygon was created to represent the outlet of the CW and, correspondingly, the most downstream point of the catchment area. The pour point was placed at the CW outlet by identifying the flow accumulation pixel with the highest value compared to neighboring pixels.

To calculate the catchment boundary, the *Watershed* tool was used with the flow direction integer raster and pour point shapefile as inputs. The output raster was then converted into a polygon. The final catchment was checked by comparing it with flow accumulation lines to see that they were extended within the same area.

### **3.1.6. Proportion of agricultural land**

The proportion of agricultural land within the catchment area was calculated using ArcMap. Data of agricultural land was obtained as a polygon shapefile from the Swedish Board of Agriculture, which consisted of registered agricultural land in 2018. The *Clip* tool was used, where the agricultural blocks were used as input and the catchments as clip features. The

areas of the catchments and agricultural land were then calculated to obtain the proportion of arable fields and pasture within each catchment. Since the catchment areas had been calculated based on the outlet of the CW, meaning that the CW area is included, the CW area was subtracted to only include the land area.

### **3.1.7. Length-to-width ratio**

The length-to-width ratios of the CWs were determined using orthophotos. The length of the CW was measured from the inlet to outlet and divided by a mean value of the CW width, which was measured every twenty meters. All measurements were performed in ArcMap. For the CWs that had two inlets, Hel and Kla, the length was measured from the inlet which was located furthest from the outlet.

### **3.1.8. Soil particle size distribution within the catchment**

The soil texture within each catchment was determined using data from The Digital Arable Soil Map of Sweden (DSMS), which contains texture data of the topsoil of agricultural land in the south of Sweden (Söderström & Piikki 2016). The map covers approximately 3 million hectares of arable land, registered by the Swedish Board of Agriculture in 2013. By the time of the survey, this corresponded to more than 90% of the total registered area of agricultural land in Sweden. The digital soil mapping is performed based on statistical modeling of soil analyses combined with available datasets, resulting in modeled values of clay and sand content in the topsoil. From the modeled values, silt content has been calculated. The generated data of soil texture is presented as raster map layers with 50 m × 50 m resolution.

The raster was processed in ArcMap. By using the *Zonal Statistics as Table* tool, mean values of the particle size distribution of agricultural land within the catchments were calculated.

### **3.1.9. Land use distribution**

The National Land Cover Database (Nationella Marktäckedata, NMD) consists of a complete map of Sweden's land cover and land use, produced by the Swedish Environmental Protection Agency in collaboration with several other agencies (Swedish Environmental Protection Agency n.d.). The NMD consist of a base layer and additional supplementary layers presented as raster with 10 m × 10 m resolution (Naturvårdsverket 2020c). Base layer data, together with a supplementary land-use layer of pasture, was collected to determine the land use distribution within the catchments (Naturvårdsverket 2020a). The land use was classified into eight categories: forest, open wetland, arable land, open land, temporary non-forest, exploited land, water, and pasture. Exploited land contains buildings, roads, and other exploited land areas, and open land consist of both land covers with and without vegetation.

The base layer raster was used as input to the *Extract by Mask* tool in ArcMap, where the catchment was used as the mask. The *Raster to Polygon* tool was thereafter used to obtain a polygon with the land-use features. The areas of the land-use categories within the catchment were then calculated. The same was executed for the pasture layer. Since pasture land overlapped with the base layer, the *Intersect* tool was used to calculate the overlapping areas. The pasture area was then subtracted from the corresponding category area which was overlapped.

### 3.5. MODELED HYDRAULIC LOADS

Hydrological data was downloaded from SMHI's water web (SMHI 2021), where water flow data were available for the years 2004 to 2019. The water flow data consists of modeled annual runoff within sub-catchments of large river basins, all computed by SMHI with the S-HYPE model set (version 16 e) (SMHI 2020). An average value of the modeled annual runoff was calculated for two time series; 2004 to 2019 and from the year of wetland construction to 2019. By knowing the average annual runoff in each sub-catchment in which the CWs and their catchments are located, Equation (2) could be implemented to retrieve the streamflow within the CW catchment. The HL of the CWs was calculated for both periods using Equation (3). The calculated HL based on long-term data (2004 to 2019) is referred to as  $HL_{LT}$ , while the construction year to 2019 is named  $HL_C$ .

Since the CW catchment areas correspond to the outlet of the CWs, calculations of streamflow become representative of the outlet. However, as most of the CWs are small in relation to their catchment area, there are no large expected differences between calculations for the inlet or outlet of the CW.

### 3.6. EROSION RISK CLASS

The erosion risk class of each catchment was determined using a modeled erosion risk map, covering over 90% of Sweden's arable land (Djordjic & Markensten 2019). The modeled risk map is based on a digital elevation model (DEM) in raster format with a resolution of  $2\text{ m} \times 2\text{ m}$ . In addition to slope variations, factors such as soil texture, water discharge, and vegetation cover were considered to calculate erosion and deposition patterns (ibid.).

Erosion risk classes were defined from 1-7, where risk class 1 implies the highest expected particle load and class 7 the lowest (Djordjic & Markensten 2019). The erosion risk map was imported to ArcMap as a shapefile. The erosion risk class of each CW was determined by the risk class that dominated the area closest to the CW.

### 3.7. MODELED PHOSPHORUS LOAD AND RETENTION

Modeled P load was available for all CWs. The modeling work was based on a DEM in raster form and calculated flow directions and flow accumulations. Each grid cell was assigned a representative export coefficient of P losses based on land use categories (Djordjic et al. 2020). For areas with arable land, the export coefficient was assigned based on the DSMS, which contains texture data of Swedish agricultural soils (Söderström & Piikki 2016; Djordjic et al. 2020). Calculated specific runoff was then multiplied with the land use-/soil-specific export coefficients to obtain P loads. The modeled loads of each grid cell were accumulated along the calculated flow pathways to determine the accumulated P load at the CW. The potential P retention was calculated using Equation (6), which is based on measured P load and retention from 15 wetlands (Weisner et al. 2015):

$$P_{ret} = (0.4584 \cdot PL) - (0.0003 \cdot PL^2) \quad (6)$$

where  $P_{ret}$  is the P retention [ $\text{kg ha}^{-1}$  wetland area  $\text{yr}^{-1}$ ] and PL is the modeled P load [ $\text{kg ha}^{-1}$  wetland area  $\text{yr}^{-1}$ ]. Equation (6) is based on measurements where the highest P retention ( $200\text{ kg ha}^{-1}\text{ yr}^{-1}$ ) was in the wetland with the highest P load ( $800\text{ kg ha}^{-1}\text{ yr}^{-1}$ ). There was no

wetland with a high P load that had a lower P retention and the polynomial fit is considered to only apply to P loads that are less than, or equal to, the largest measured load in the study.

### **3.8. SEDIMENT SAMPLING**

The sediment sampling of the ten CWs was performed during March 2021. Sediment cores were collected at the inlet and outlet of each CW. For those wetlands with two inlets (Hel and Kla), an additional sediment core was collected at the second inlet. For the P-wetlands (Ull, Nyb, and Hos) designed with a deeper sedimentation basin followed by a shallow vegetation zone, a total of four samples were taken; at the inlet, at the end of the sedimentation basin, at the beginning of the vegetation zone, and the outlet of the CW.

The sediment cores were collected with a Willner gravity corer with plexiglass tubes of 50 cm long and 10 cm in diameter (Figure 4). The instrument was lowered into the water and pushed down into the sediment as far as possible until the clay bottom of the CW was reached.

Samples were collected both by wading into the water and by boat. Samples collected by boat were:

- Inlets in Okn 2, Hos, Mar, Kla, and Nyb.
- At the end of the sedimentation basin in Hos and Nyb.
- Outlets in Okn 2, Hel, Kla, and Ste.

The Ull wetland had an ice cover on the water surface when the samples were collected and the ice had to be chopped in order to lower the Willner gravity corer into the water.

The water level and sediment depth were measured next to the sampling point by using a measuring stick. The stick was lowered into the water until reaching the top of the sediment, followed by inserting the stick into the sediment to determine the sediment depth.



*Figure 4. Sediment cores collected at the outlet of the CW Ste. The brown layers are accumulated sediment, which varies between 26 and 36 cm. The clay bottom of the CW can be seen in the bottom 6-7 cm of the tube (grey layer). The left sediment core was selected for P analysis, and the core to the right was analyzed regarding the particle size distribution (which is not included in the scope of this project). Photo: Gabriella Corbee.*

The accumulated sediment was sliced into a plastic jar one centimeter at a time until the lower clay bottom layer was reached. The samples were delivered to SLU and stored in a refrigerated room until the P analysis was performed by the geochemistry laboratory, Department of water and environment at SLU.

Two particularly notable observations made during the fieldwork were at the Hel wetland. It was noticed that the arable land along the west side of Hel was plowed down to the shore in some areas (Figure 5). Moreover, indications of shore erosion could be observed in areas close to the outlet.



Figure 5. To the left, the arable land along the west shore of Hel, which in some areas was plowed all the way down to the water. The right photograph shows the shoreline in an area close to the outlet point. Photo: Gabriella Corbee.

### 3.9. PHOSPHORUS ANALYSIS

The laboratory analysis was performed by the geochemistry laboratory (SLU) using a chemical extraction method for wet sediment according to Lannergård et al. (2020). The sediment samples were homogenized and sieved (1 mm), followed by placing a known amount of sediment into a centrifuge tube to be sequentially extracted. In each extraction step, an extractant (10 ml) was added to the sample and the reaction between extractant and sediment was allowed to proceed for a given time. The following sequential extractions were performed to quantify the P fractions in sediment:

- P in pore water (PW-P) with extractant H<sub>2</sub>O (double de-ionized water) for 2 hr.
- Iron-bound P (Fe-P) with extractant Na<sub>2</sub>SO<sub>3</sub>/NaHCO<sub>3</sub> (0.11 mol/L) for 10 min followed by a second 1-hr extraction.
- Aluminum-bound P (Al-P) with extractant NaOH (1 mol/L) for 16 hr.
- Organically bound P (Org-P) with the addition of potassium persulfate and autoclaved for 16 hr.
- Calcium-bound P (Ca-P) with extractant HCl (0.5 mol/L) for 16 hr.

Three blank samples were run in each sample batch for quality control. Moreover, every analysis batch included a reference sample for the identification of possible discrepancies between runs.

The water content in the sediment samples was determined by freezing the samples for 12 hr (-20°C) followed by freeze-drying for 96 hr (-40°C). A loss of ignition test was performed for 2 hr (550°C), followed by determining the percent organic matter and bulk density of the sediment. The bulk density was calculated with Equation (7) (Lannergård et al. 2020):

$$\rho = \frac{260}{100 + 1.6 \cdot (W + \left(\frac{100 - W}{100}\right) \cdot IG)} \quad (7)$$

where  $\rho$  is the bulk density [ $\text{g cm}^{-3}$ ],  $W$  is the water content [%] and  $IG$  is the organic matter content [%]. The concentration of each P fraction in dry soil [ $\text{mg g}^{-1}$ ] was determined based on the amount of P extracted from the sediment. Moreover, the amount of P fraction per volume of dry soil [ $\text{mg cm}^{-3}$ ] was determined based on the soil concentration, bulk density, and dry matter content.

### 3.10. TOTAL PHOSPHORUS AND PARTICLE ACCUMULATION IN SEDIMENT

The total P (TP) in sediment [ $\text{mg cm}^{-3}$ ] could be determined (from the results of the P analysis) by summing the amount of each P fraction per volume of dry soil (Equation (8)).

$$TP = PWP + FeP + ALP + OrgP + CaP \quad (8)$$

The TP for each sliced sample was then calculated by multiplying TP with the sample depth [cm]. The sliced accumulation layers were summed up to obtain the TP for each sampled sediment core [ $\text{mg cm}^{-2}$ ]. A mean value of TP for the cores collected in each CW was then calculated and multiplied with the surface area of the CW to obtain TP accumulation [kg]. By knowing CW age and area, the annual accumulation of TP per ha CW area could be determined [ $\text{kg ha}^{-1} \text{yr}^{-1}$ ].

The total amount of particles that have settled in the wetlands was estimated by multiplying the bulk density with the sediment fraction and sample depth of each sliced sample. The accumulation layers were summed up to obtain the dry weight (DW) in each sampled core, of which an average value was calculated and multiplied with the CW surface area to obtain DW accumulation in tonnes [t]. The DW of settled particles per ha CW area and year could then be determined [ $\text{t ha}^{-1} \text{yr}^{-1}$ ].

### 3.11. STATISTICAL ANALYSIS

The statistical software Minitab was used for all statistical analyses. Simple regression analyses were performed to examine the correlation between potential influencing factors and the total particle and P accumulation. The following factors were evaluated: CW area, L:W ratio, water depth,  $A_W:A_C$  ratio, the proportion of agricultural land, clay fraction in the topsoil,  $HL_{LT}$ , P load, calculated P retention, and erosion risk class. The  $HL_C$  (construction year to 2019) was excluded from the regression analyses since three of the CWs were constructed before the earliest year of which flow data was available.

Regression analyses were performed with a level of significance of 95% ( $p < 0.05$ ). The accumulation was set as the response variable, while the potential influencing factors were set as predictors. The regression fits are linear unless stated otherwise in the results.

Additionally, ANOVA (analysis of variance) and Tukey's pairwise comparison method were used to determine if it was a significant difference between the P-wetlands and ponds regarding annual sediment accumulation and P accumulation.

## 4. RESULTS

### 4.1. HYDRAULIC LOADS, EROSION RISK CLASS, AND MODELED P LOADS

Based on average annual values of discharge, HL was determined for two time series. With long-term data from 2004 to 2019 ( $HL_{LT}$ ), the obtained loads vary in a range from 2 to 854  $m\ yr^{-1}$  (Table 2). Hos had the largest  $HL_{LT}$ , followed by Okn 1 (448  $m\ yr^{-1}$ ). However, when considering the total wetland area of Okn, the  $HL_{LT}$  was 48  $m\ yr^{-1}$ . With discharge data from the construction year to 2019, the  $HL_C$  was generally smaller except for Okn 2. The  $HL_C$  ranged from 2 to 697  $m\ yr^{-1}$ . The CWs with the largest surface areas (Hel, Kla, Ste, and Mar) had the smallest HL, which is in accordance with what can be expected from Equation (3) since the HL is annual flow divided by CW area.

The erosion risk class for the CWs was determined based on the modeled risk maps presented in Appendix A.3. No CW was found to be situated in areas with the highest risk of erosion, which corresponds to risk class 1. The majority of the CWs are at medium/medium-high risk of erosion, located in areas with risk classes 3 and 4 (Table 2). Kla and Ste were classified within risk 5, which means that they can be expected to have the smallest particle load of all CWs.

The modeled P load was evaluated regarding the influence of erosion risk class, the proportion of clay in topsoil, and agricultural land in the catchment. Linear regression analyzes did however not indicate any correlation between P load and the factors; erosion risk class ( $R^2 = 11.4\%$ ,  $p = 0.34$ ), proportion of clay ( $R^2 = 0.21\%$ ,  $p = 0.89$ ), proportion of agricultural land ( $R^2 = 3.7\%$ ,  $p = 0.59$ ). The modeled P load, which is based on specific runoff, did however show a strong correlation to the  $HL_{LT}$  (polynomial trend  $R^2 = 98.7\%$ ,  $p < 0.001$ ).

Considering the modeled P load, Hos is expected to receive the largest amount of P per wetland area with a load of 2480  $kg\ P\ ha^{-1}\ yr^{-1}$ . Given this large load, a negative potential P retention was estimated using Weisner's polynomial equation (6). However, until reaching the breaking point of where negative retention is obtained, a larger P load leads to a greater potential P retention. This can be seen in Table 2, where Okn 1 has the second-largest P load (639  $kg\ ha^{-1}\ yr^{-1}$ ) and therefore the greatest expected P retention (170  $kg\ ha^{-1}\ yr^{-1}$ ). It should be noted that the P load in Hos (2480  $kg\ ha^{-1}\ yr^{-1}$ ) exceeds the largest measured P load (800  $kg\ ha^{-1}\ yr^{-1}$ ) which Weisner's equation is based on. Weisner's equation is therefore not applicable to give a reliable estimation of the potential P retention in Hos wetland.

Table 2. Modeled HL based on average annual discharge for two time series; long-term from 2004 to 2019 ( $HL_{LT}$ ) and from the year of wetland construction to 2019 ( $HL_C$ ). Fields with “-“ indicates that the modeled time series cannot be applied to the CW. The modeled P load (PL), potential P retention (Pot.  $P_{ret}$ ), and erosion risk class are also presented.

CW	$HL_{LT}$ [m yr <sup>-1</sup> ]	$HL_C$ [m yr <sup>-1</sup> ]	PL [kg ha <sup>-1</sup> yr <sup>-1</sup> ]	Pot. $P_{ret}$ [kg ha <sup>-1</sup> yr <sup>-1</sup> ]	Erosion risk class
Okn	47.8	- <sup>c</sup>			4
Okn 1	448	410	639	170	4
Okn 2	53.4 <sup>a</sup>	- <sup>d</sup>	75.5	32.9	4
Hos	854	697	2480	-711 <sup>b</sup>	3
Nyb	211	208	351	124	3
Okn S	139	128	265	100	4
Ull	143	145	291	108	3
Mar	6.35	5.85	17.3	7.82	3
Kla	3.54	- <sup>d</sup>	6.51	2.97	5
Hel	2.29	2.13	3.63	1.66	3
Ste	2.45	- <sup>d</sup>	4.60	2.10	5

a. Calculated based on the total catchment area of both Okn 1 and 2.

b. A negative value was obtained (Equation (6)) as a result of a high modeled P load per hectare CW area.

c. Okn consists of two connected wetlands constructed in different years.

d. Okn 2, Kla, and Ste are constructed before the earliest year of which flow data is available.

#### 4.2. SEDIMENT CHARACTERIZATION

The color of the collected sediment cores differed considerably for some CWs, while others had a relatively homogeneous accumulation layer throughout the whole CW area. Most CWs had darker sediment at the outlets (Table 3). However, this was not observed in four of the CWs (Hos, Nyb, Okn S, Ull) which all had the same, or lighter, colored sediment at the outlet compared to the other CW sections where cores were collected. Most of the sampled cores had an accumulation layer in different shades of brown and brown-grey. Some CWs were also observed to have elements of black accumulated sediment in the collected cores; Okn 1 (outlet), Okn 2 (outlet), Hos (inlet, out D), Nyb (out D), Mar (inlet, outlet), and Kla (upper inlet, outlet). Orange elements of Fe-precipitate were observed in the sediment of Okn 1's inlet and at the end of the sedimentation basin in Ull. Moreover, the accumulation layer of the sediment cores from Kla, Hel, and Ste was observed to contain a great amount of what appeared to be lumpy (aggregated) clay.

The OM in sediment varied greatly between the sampling points in some of the CWs (Table 3). Okn 1 had more OM in the sediment at the outlet (14%) together with a lower bulk density (1.2 g cm<sup>-3</sup>) than at the initial area of the wetland (6% and 1.4 g cm<sup>-3</sup>). Okn S and Kla also had more OM in the outlet section. In Hos, the OM varied between 4 and 16%, with the largest share of OM at the beginning of the vegetation section. However, the bulk density was the same for the section with the lowest and largest OM. Both Ull and Mar had more OM in the initial area of the wetland compared to the outlet.

Table 3. Sediment characterization with the color of the accumulated sediment, the bulk density of the sediment ( $\rho$ ), and organic matter content of sediment (OM) obtained from the P analysis. The water depth at each CW section is also presented.  $\rho$  and OM are average values of the sliced accumulation layers in the sediment core.

CW	Section	Water depth [m]	Color	$\rho$ [g cm <sup>-3</sup> ]	OM [%]
Okn 1	Inlet	0.3	Brown, orange	1.4	6
	Outlet	0.6	Brown, grey/black	1.2	14
Okn 2	Inlet	0.3	Brown, dark grey	1.1	23
	Outlet	2.8	Dark brown, grey/black	1.1	22
Hos	Inlet	1	Brown, black	1.4	4
	Out D	1	Brown, black	1.2	6
	In V	0.3	Light brown	1.4	16
	Outlet	0.3	Brown, dark grey	1.3	5
Nyb	Inlet	0.5	Brown, grey	1.4 <sup>a</sup>	7 <sup>a</sup>
	Out D	0.7	Brown, grey, black	1.5 <sup>a</sup>	6 <sup>a</sup>
	In V	0.2	Brown, grey	1.5 <sup>a</sup>	7 <sup>a</sup>
	Outlet	0.2	Brown, grey	1.4 <sup>a</sup>	7 <sup>a</sup>
Okn S	Inlet	0.4	Orange-brown, dark brown	1.3 <sup>a</sup>	10 <sup>a</sup>
	Outlet	0.2	Orange-brown, brown	1.4 <sup>a</sup>	16 <sup>a</sup>
Ull	Inlet	0.5	Brown, dark brown	1.2	23
	Out D	0.7	Brown, dark brown, orange	1.2	11
	In V	0.2	Light brown	1.2	20
	Outlet	0.3	Light brown, dark brown	1.3	10
Mar	Inlet	1.8	Light brown, black	1.1	20
	Outlet	1.1	Brown, black	1.3	5
Kla	Inlet (upper)	0.5	Brown/grey, black	1.1	17
	Inlet (lower)	0.5	Brown	1.1	15
	Outlet	1	Dark brown/black	1.2	20
Hel	Inlet (upper)	0.5	Light brown, brown	1.5	8
	Inlet (lower)	0.4	Light brown, brown	1.4	11
	Outlet	1.1	Brown, brown-grey	1.4	9
Ste	Inlet	0.4	Brown	1.2	26
	Outlet	0.6	Brown, dark brown-grey	1.1	26

a. Sediment analysis results of sediment cores collected in April and May 2020.

### 4.3. ANNUAL SEDIMENT ACCUMULATION

The average annual sediment accumulation [ $\text{cm yr}^{-1}$ ] measured from the sampled cores is presented in Figure 6. The accumulation is a mean value of the sediment cores (one analyzed for P and one regarding the particle size distribution in sediment, Figure 4). Since the boundary between the accumulation layer and bottom layer could be difficult to distinguish, the value has also been corrected based on what was sliced and sent for analysis.

The P-wetland Nyb had the highest sedimentation, with an average of  $2.4 \text{ cm yr}^{-1}$  (Figure 6). The two other P-wetlands, Hos and Ull, had the second and third lowest accumulation of all wetlands;  $0.6$  and  $0.8 \text{ cm yr}^{-1}$ , respectively. The second-highest accumulation was found in Hel, where the mean value of accumulated sediment was  $1.6 \text{ cm yr}^{-1}$ . Kla had the lowest sedimentation of all wetlands, with an average of  $0.3 \text{ cm yr}^{-1}$ . Okn 1 had an annual accumulation of  $1.3 \text{ cm yr}^{-1}$ , Okn 2 had  $0.8 \text{ cm yr}^{-1}$ , and the average accumulation of the two connected wetlands together was  $1.1 \text{ cm yr}^{-1}$ .

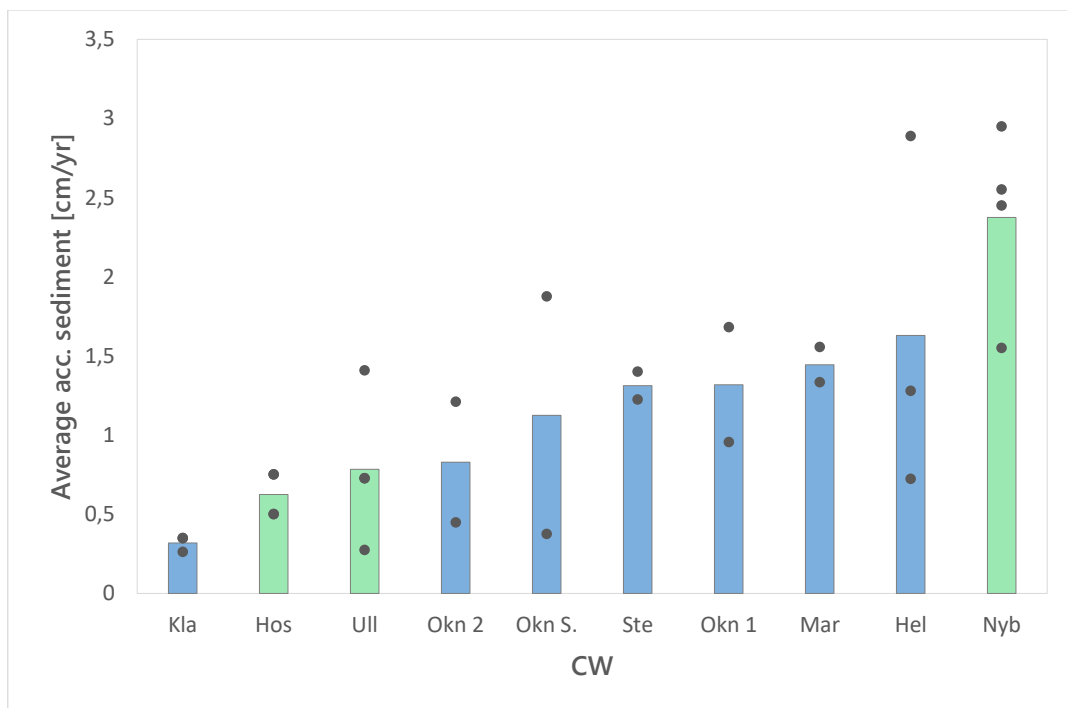


Figure 6. Mean values of measured accumulated sediment [ $\text{cm yr}^{-1}$ ] in sampled cores for all sampling points in the wetlands; ponds (blue bars) and P-wetlands (green bars). Filled circles indicate the variation within the CW.

The difference in average sediment accumulation between the two wetland types is illustrated in Figure 7. The P-wetlands ( $n = 3$ ) had a mean value of  $1.3 \text{ cm yr}^{-1}$  and a median of  $0.8 \text{ cm yr}^{-1}$ . For the ponds ( $n = 7$ ), the mean value was  $1.1 \text{ cm yr}^{-1}$  and the median was  $1.3 \text{ cm yr}^{-1}$ . Hence, the mean values of accumulation in the two wetland types are relatively equal. Tukey's pairwise comparison showed that there was no significant difference between the wetland types.

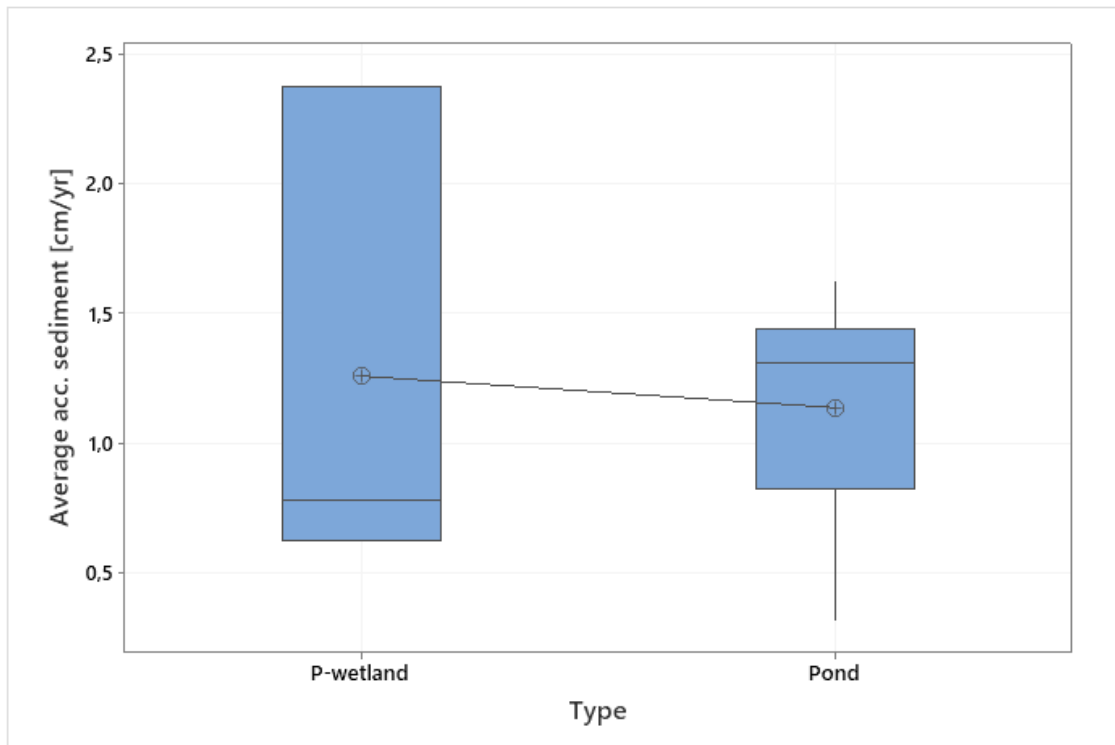


Figure 7. Boxplot of average annual accumulation in the different wetland types; P-wetlands ( $n = 3$ ), ponds ( $n = 7$ ). The horizontal line represents the median, circled cross the mean value. The upper and lower edge of the box represents the quartiles. The vertical lines (whiskers) go from the quartiles to the maximum (top) or minimum accumulation (bottom).

When comparing the sampling points, there was a large variation in how much sediment had accumulated within the CWs (Figure 8). Hel, Mar, and Ste had more sediment at the outlet of the wetland than at the inlet, where the largest difference was found in Hel. The accumulation at Hel's outlet was found to be over  $1.5 \text{ cm yr}^{-1}$  more than the accumulation occurring at the inlets. Kla, Nyb, Okn 1, Okn 2, and Okn S all had a higher accumulation at the inlets. Moreover, Kla had the same measured amount of accumulated sediment at both inlets ( $0.35 \text{ cm yr}^{-1}$ ).

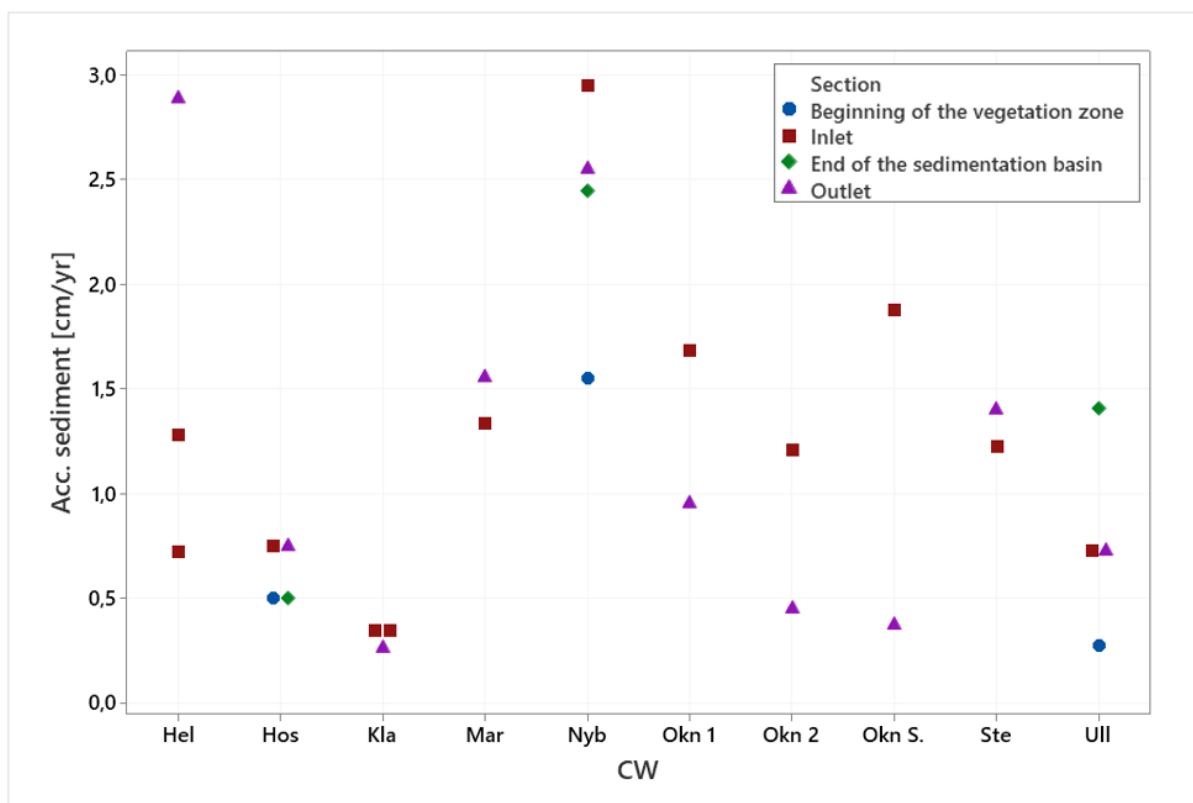


Figure 8. The accumulated sediment in each sampling point per year. Samples were collected at the inlets (red squares), outlets (purple triangles), where the vegetation zone starts (blue circles), and at the end of the deep section (green rhombs). For Hel, the inlet from an open ditch had more annual accumulation than the inlet from a drainage pipe.

When looking at the P-wetlands divided into deep and shallow vegetated sections (Hos, Nyb, and Ull), there does not seem to be any distinct accumulation pattern of the different wetland zones (Figure 8). The P-wetland Hos had the same measured amount of accumulated sediment in the inlet and outlet ( $0.75 \text{ cm yr}^{-1}$ ). The sampling points at the end of the deep section and the start of the vegetation section both measured an accumulation of  $0.5 \text{ cm yr}^{-1}$ . For Nyb, the largest accumulation was found at the inlet ( $2.95 \text{ cm yr}^{-1}$ ), followed by the outlet ( $2.55 \text{ cm yr}^{-1}$ ) which was slightly higher than the end of the deep section ( $2.45 \text{ cm yr}^{-1}$ ). The sampling point where the vegetation zone starts had  $1.55 \text{ cm yr}^{-1}$  in Nyb. For Ull, it was instead at the end of the deeper section where most sediment had accumulated ( $1.41 \text{ cm yr}^{-1}$ ). The in- and outlet in Ull had the same accumulation ( $0.73 \text{ cm yr}^{-1}$ ), while the smallest accumulation had occurred at the beginning of the vegetation section ( $0.27 \text{ cm yr}^{-1}$ ).

The depth of the sediment accumulation in the CWs was estimated both by inserting a measuring stick into the sediment and by measuring the sampled sediment core. The relationship between the two measurement methods was found to be statistically significant;  $R^2 = 45.5\%$  and  $p < 0.001$  (Figure 9). The linear regression fit was:

$$\text{Sediment depth (sample)} = 4.317 + 0.2686 \cdot \text{Sediment depth (stick)} \quad (9)$$

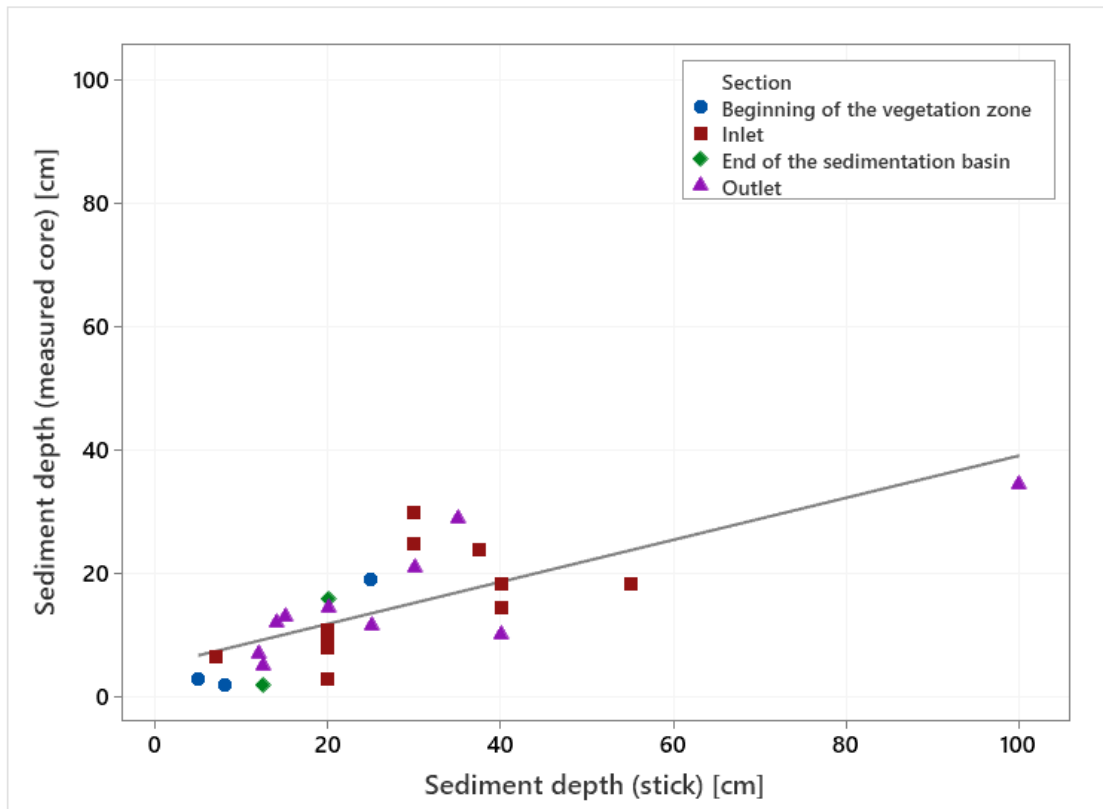


Figure 9. Linear regression of sediment depth measured with a stick into the sediment in relation to the collected sediment core (accumulation depth of what was sliced and sent for analysis).  $R^2 = 45.5\%$ ,  $p < 0.001$ . Samples were collected at the inlets (red squares), outlets (purple triangles), where the vegetation zone starts (blue circles), and at the end of the deep section (green rhombs).

Considering the water depth at the sampling points and the potential correlation to sediment accumulation per year, no trend could be seen ( $R^2 = 0.72\%$ ,  $p = 0.67$ , Figure 10).

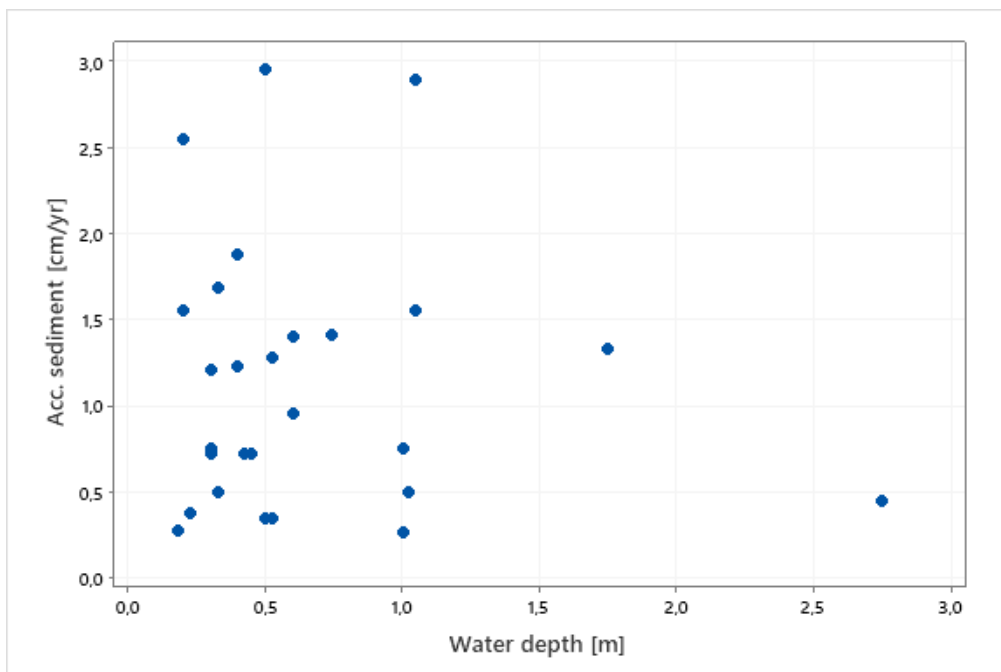


Figure 10. Accumulated sediment at different water depths.

The accumulation was also evaluated divided by samples taken at water depths greater than 1 m and depths less than 0.4 and 1 m. Even in these cases, no connection between water and sediment depth could be established. Furthermore, the accumulation in the P-wetlands in relation to the water depth was examined but no correlation could be detected.

#### 4.4. TOTAL PHOSPHORUS AND PARTICLE ACCUMULATION

The total amount of particles that have settled in the CWs varied between 7 and 130 t ha<sup>-1</sup> yr<sup>-1</sup> (Table 4). Hel had the largest amount of settled particles per year relative to its area, followed by Nyb (100 t ha<sup>-1</sup> yr<sup>-1</sup>). The smallest DW was found in Kla, while Mar had the second smallest amount of settled particles (14 t ha<sup>-1</sup> yr<sup>-1</sup>). Okn S had the largest P accumulation of all wetlands (96 kg ha<sup>-1</sup> yr<sup>-1</sup>), followed by Hel (80 kg ha<sup>-1</sup> yr<sup>-1</sup>). It should be noted that the P accumulation in Okn S exceeds Hel, even though the total particle sedimentation in Okn S (60 t ha<sup>-1</sup> yr<sup>-1</sup>) is less than half of the particle amount that has settled in Hel. However, the total P concentration in the sediment of Okn S was more than three times higher than in Hel (1900 and 600 mg kg<sup>-1</sup>, respectively). The smallest amount of accumulated P was found in Mar and Kla (8 kg ha<sup>-1</sup> yr<sup>-1</sup>), where Mar had twice as much DW accumulation as Kla (14 and 7 t ha<sup>-1</sup> yr<sup>-1</sup>, respectively). However, the P concentration was 600 mg kg<sup>-1</sup> in Mar and 2000 mg kg<sup>-1</sup> in Kla.

Table 4. The total amount of accumulated particles (DW), total P accumulation in wetland sediment (TP accumulation), and total P concentration in wetland sediment (TP concentration).

CW	DW [t ha <sup>-1</sup> yr <sup>-1</sup> ]	TP accumulation [kg ha <sup>-1</sup> yr <sup>-1</sup> ]	TP concentration [mg kg <sup>-1</sup> ]
Mar	14	8	600
Kla	7	8	2000
Ull	26	10	400
Hos	31	18	600
Okn 2	19	37	1000
Okn 1	63	38	700
Ste	35	38	1100
Nyb	100	69	700
Hel	130	80	600
Okn S	60	96	1900

The correlation between P accumulation and particle accumulation is presented in Figure 11. The variables are positively correlated to each other with a statistically significant linear trend with R<sup>2</sup> = 61.8% and p = 0.007. No correlation could be observed between P accumulation and P concentration in wetland sediment (R<sup>2</sup> = 4.6%, p = 0.55). Hence, the P accumulation is mainly correlated to the particle accumulation and not the P concentration.

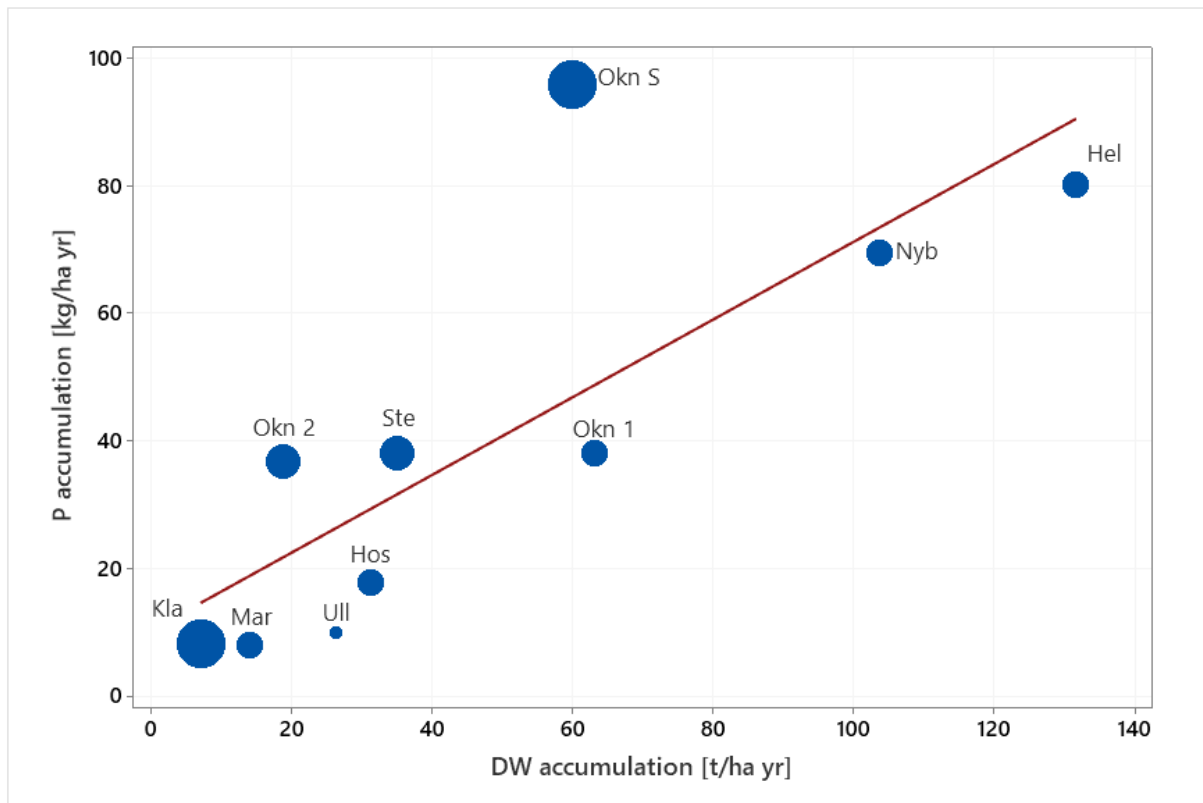


Figure 11. Total P accumulation in relation to the total particle accumulation,  $R^2 = 61.8\%$ ,  $p = 0.007$ . The size of the circles indicates the P concentration in sediment, where a large circle corresponds to a high concentration.

The difference in P accumulation between the two wetland types is illustrated in Figure 12. For the P-wetlands, the mean value of P accumulation was  $32 \text{ kg ha}^{-1} \text{ yr}^{-1}$  and the median  $18 \text{ kg ha}^{-1} \text{ yr}^{-1}$ . The ponds had an average P accumulation of  $44 \text{ kg ha}^{-1} \text{ yr}^{-1}$  and a median of  $38 \text{ kg ha}^{-1} \text{ yr}^{-1}$ . Tukey's pairwise comparison divided the two wetland types within the same grouping, indicating no differences of means. Moreover, no statistical significance was obtained in the variance analysis ( $p = 0.638$ ), meaning that there was no significant difference between the wetland types. Tukey's pairwise comparison was also performed regarding the DW accumulation and P concentration in sediment but no significant difference between the wetland types was detected.

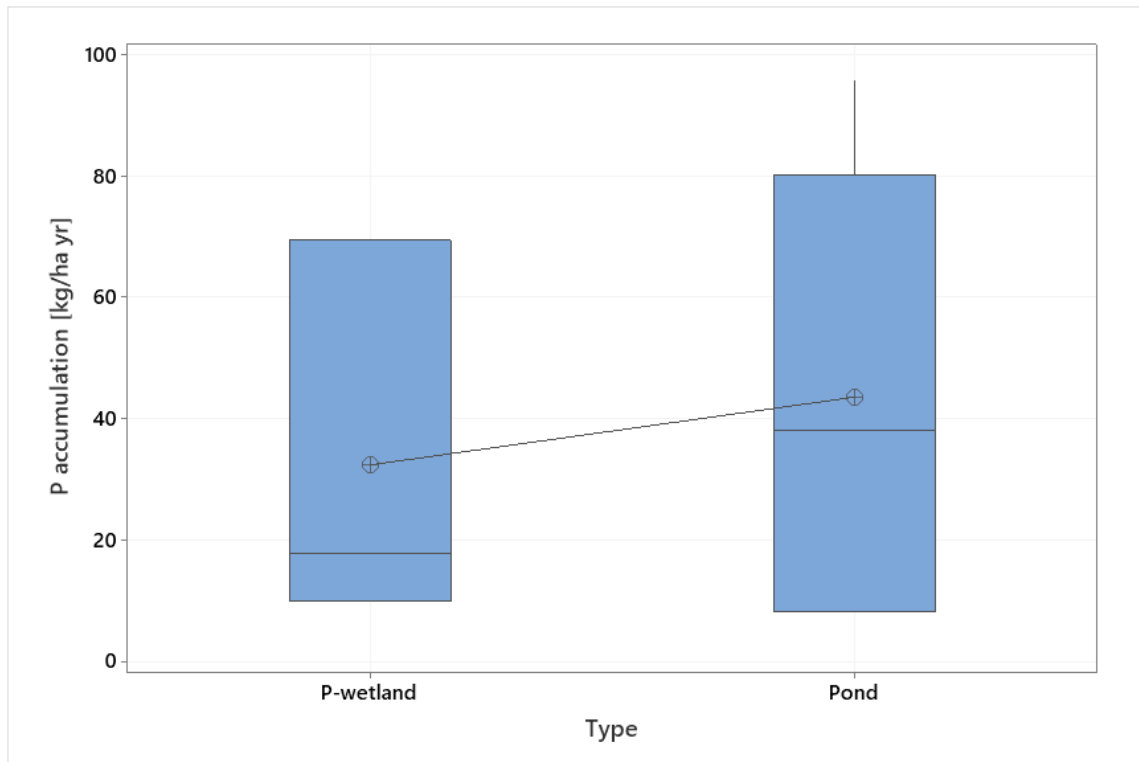


Figure 12. Boxplot of P accumulation in the different wetland types; P-wetlands (n = 3), ponds (n = 7). The horizontal line represents the median, circled cross the mean value. The upper and lower edge of the box represents the quartiles. The vertical line (whisker) goes from the quartile to the maximum P accumulation.

#### 4.4.1. Wetland design and relative size to catchment affecting P and DW accumulation

None of the evaluated wetland design factors showed any correlation to the total P accumulation; CW area ( $R^2 = 2.7\%$ ,  $p = 0.65$ ), L:W ratio ( $R^2 = 1.0\%$ ,  $p = 0.78$ ), and water depth ( $R^2 = 4.4\%$ ,  $p = 0.29$ ). It could however be observed that the P accumulation was low in deep water areas  $> 1.5$  m, while water depths up to approximately 1 m resulted in a large variety of accumulated P. The CW area, L:W and water depth showed no correlation to the DW accumulation. However, when excluding the CWs with the extremely large (Hel) and extremely small (Kla) particle accumulation, a statistically significant linear trend was observed for the DW accumulation in relation to the L:W ratio ( $R^2 = 59.6\%$ ,  $p = 0.025$ , Figure 13).

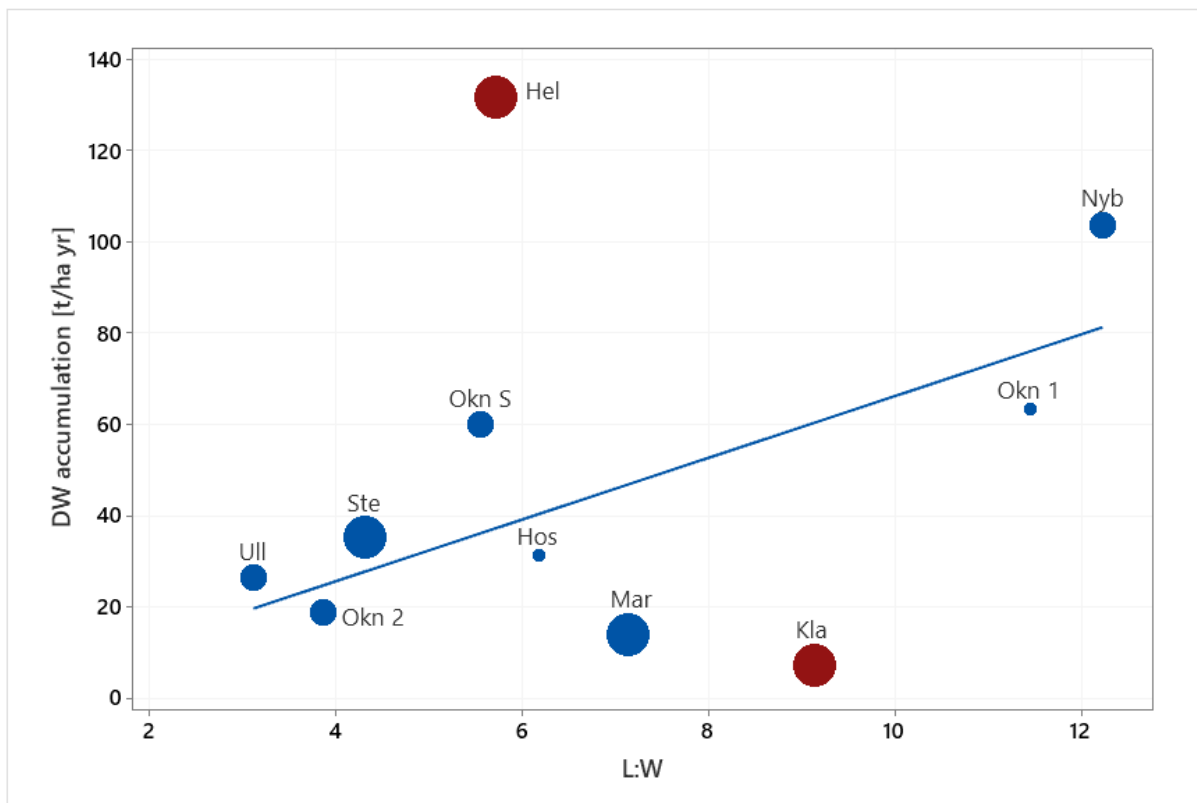


Figure 13. The total particle accumulation in the wetlands in relation to the L:W ratio. With Hel and Kla excluded (red circles):  $R^2 = 59.6\%$ ,  $p = 0.025$ . The size of the circles indicates the  $A_C:A_W$  ratio;  $<0.1\%$  (small circles),  $0.1\% < A_C:A_W < 1\%$  (medium circles),  $>1\%$  (large circles).

The relationship between the P accumulation and CW area relative to the catchment area is presented in Figure 14. No correlation could be observed for the studied data, nor could a correlation be observed for the particle accumulation in relation to the  $A_W:A_C$  ratio (Figure 15). The P accumulation in the CWs with a smaller ratio ( $< 0.4\%$ ) varied between 10 and 96  $\text{kg ha}^{-1} \text{yr}^{-1}$ . Notable is that the smallest and largest P accumulation was found in Ull and Okn S CWs, which have a similar  $A_W:A_C$  ratio (0.16 and 0.14%). Moreover, similar P accumulation patterns could be observed in Ste ( $A_W:A_C$  7%) as for CWs with relative size to the catchment of 0.04% (Okn 1) and 0.35% (Okn 2). Due to the potential erosion that contributed to the particle accumulation at the outlet in Hel, the P and DW accumulation at the inlets was also examined to see if a more evident relation could be observed between the variables. However, no correlation could be observed between the accumulation at the inlet and the  $A_W:A_C$  ratio.

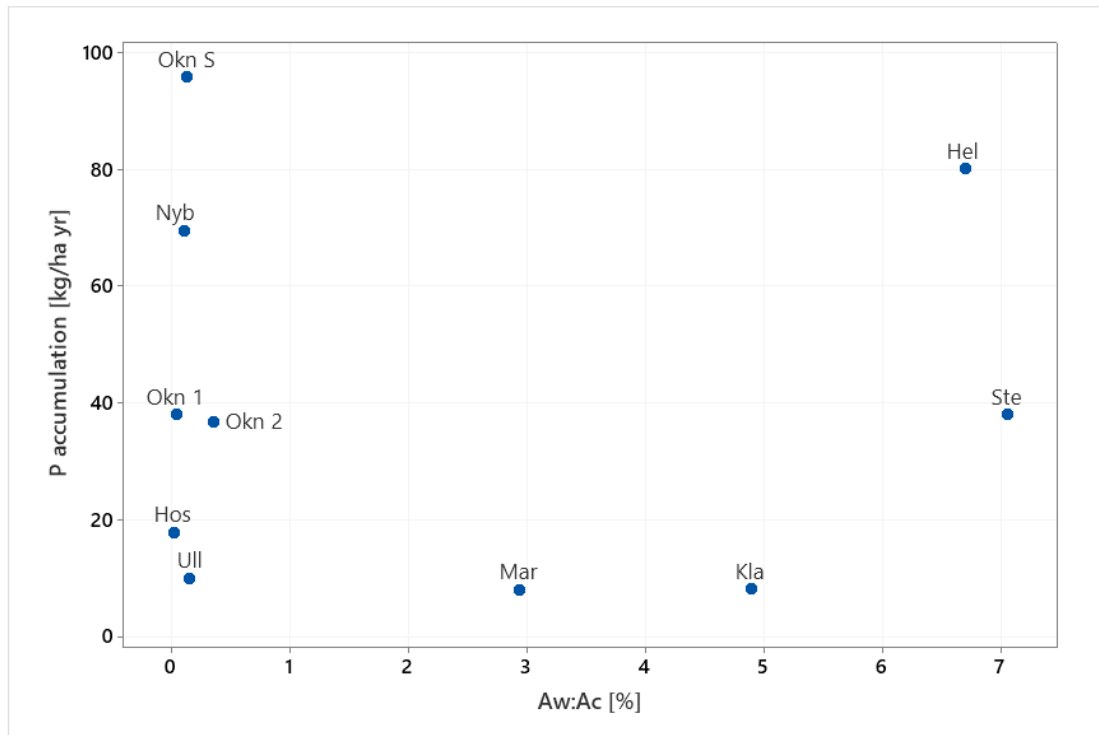


Figure 14. The total P accumulation in relation to the  $A_w:A_c$  ratio.

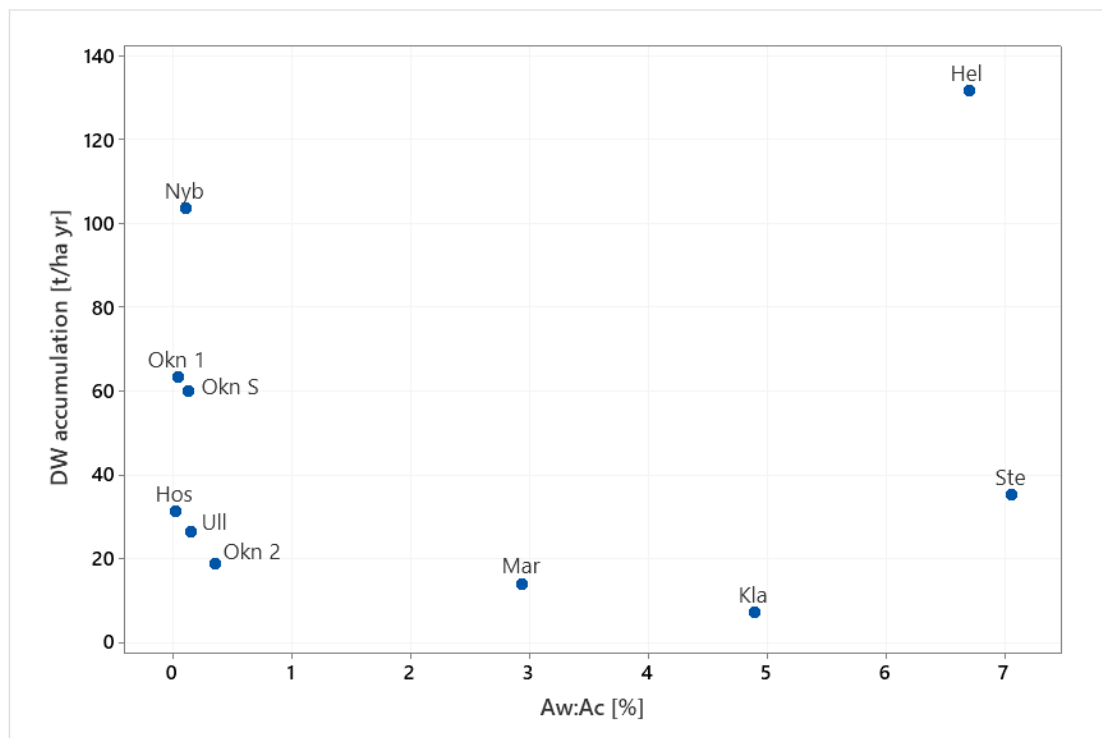


Figure 15. The total particle accumulation in relation to the  $A_w:A_c$  ratio.

#### 4.4.2. Proportion of agricultural land and clay content in the catchment area affecting P and DW accumulation

The proportion of agricultural land within each catchment was evaluated regarding the P and DW accumulation, but no correlation could be observed. The clay content in the topsoil did

however show a statistically significant correlation to both the P accumulation ( $R^2 = 46.2\%$ ,  $p = 0.031$ , Figure 16) and DW accumulation ( $R^2 = 40.9\%$ ,  $p = 0.047$ , Figure 17). Hence, an increased share of clay seems to have a positive influence on the total P and particle accumulation in the wetlands, resulting in an increased accumulation.

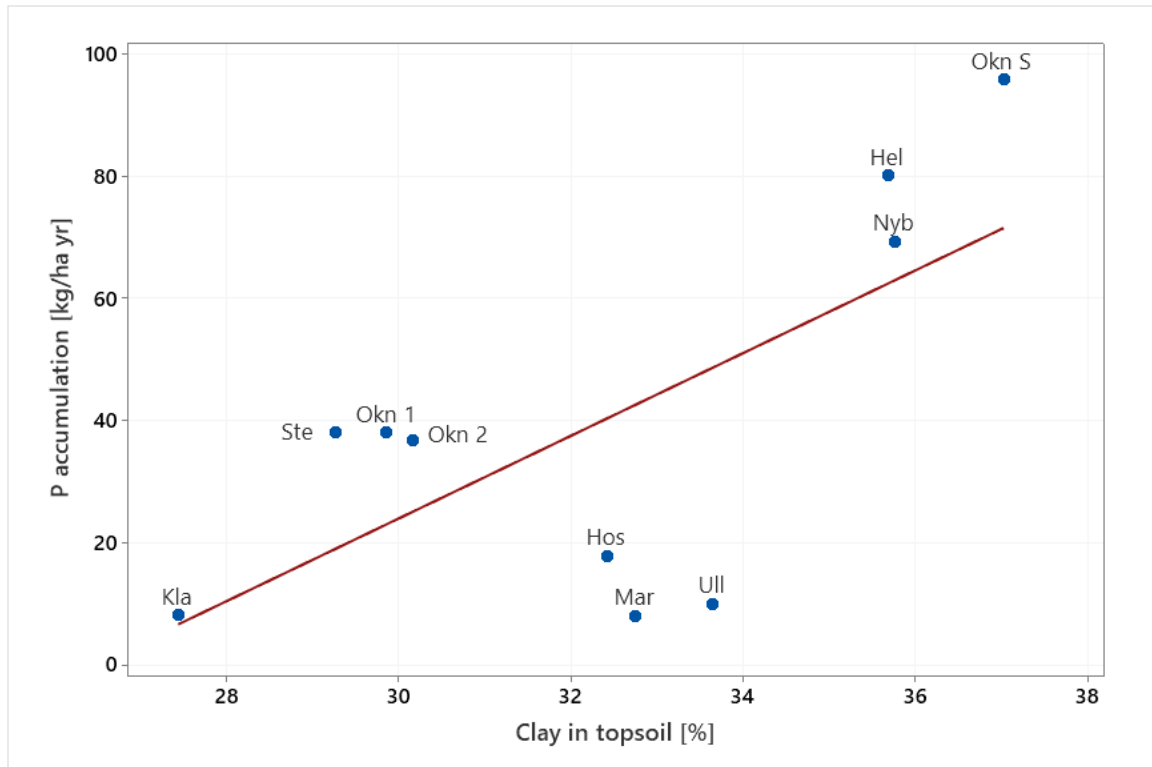


Figure 16. The P accumulation in relation to the clay content in the topsoil of the catchment. Linear regression line with  $R^2 = 46.2\%$ ,  $p = 0.031$ .

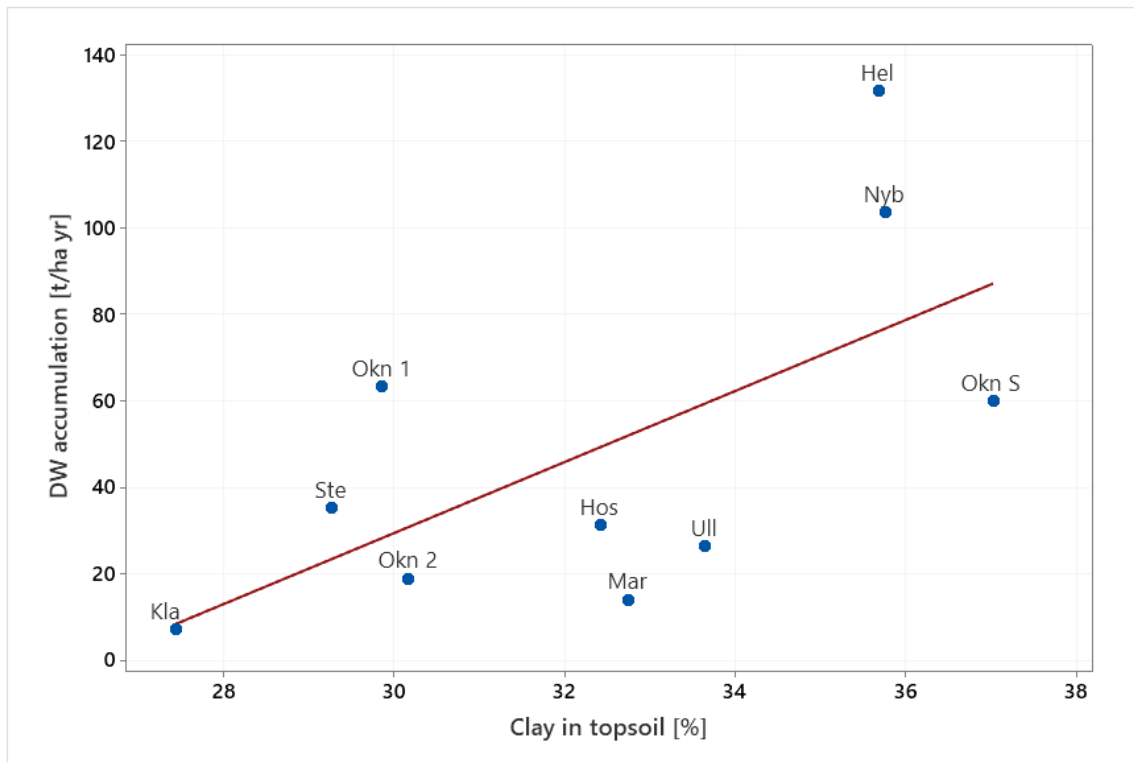


Figure 17. The total particle accumulation in relation to the clay content in the topsoil of the catchment. Linear regression line with  $R^2 = 40.9\%$ ,  $p = 0.047$ .

#### 4.4.3. Modeled loads and erosion risk class affecting P and DW accumulation

The measured P accumulation and the potential P retention based on modeled P load are presented in Figure 18. The potential P retention was shown to be a good estimation for four of the wetlands; Kla, Mar, Okn 2, and Okn S. However, the regression analysis showed no correlation between measured and potential values of accumulated P ( $R^2 = 7.95\%$ ,  $p = 0.43$ ). No correlation could be observed between measured P accumulation and the P load either (polynomial fit  $R^2 = 10.2\%$ ,  $p = 0.69$ ). For Nyb, Okn 1, and Ull, the potential P retention in the wetland was highly overestimated compared to what was accumulated based on the sampled sediment cores. Hel, Hos, and Ste accumulated more P than what was estimated based on the P load. It should however be noted that a negative potential P retention in Hos was estimated based on Weisner's polynomial equation (6).

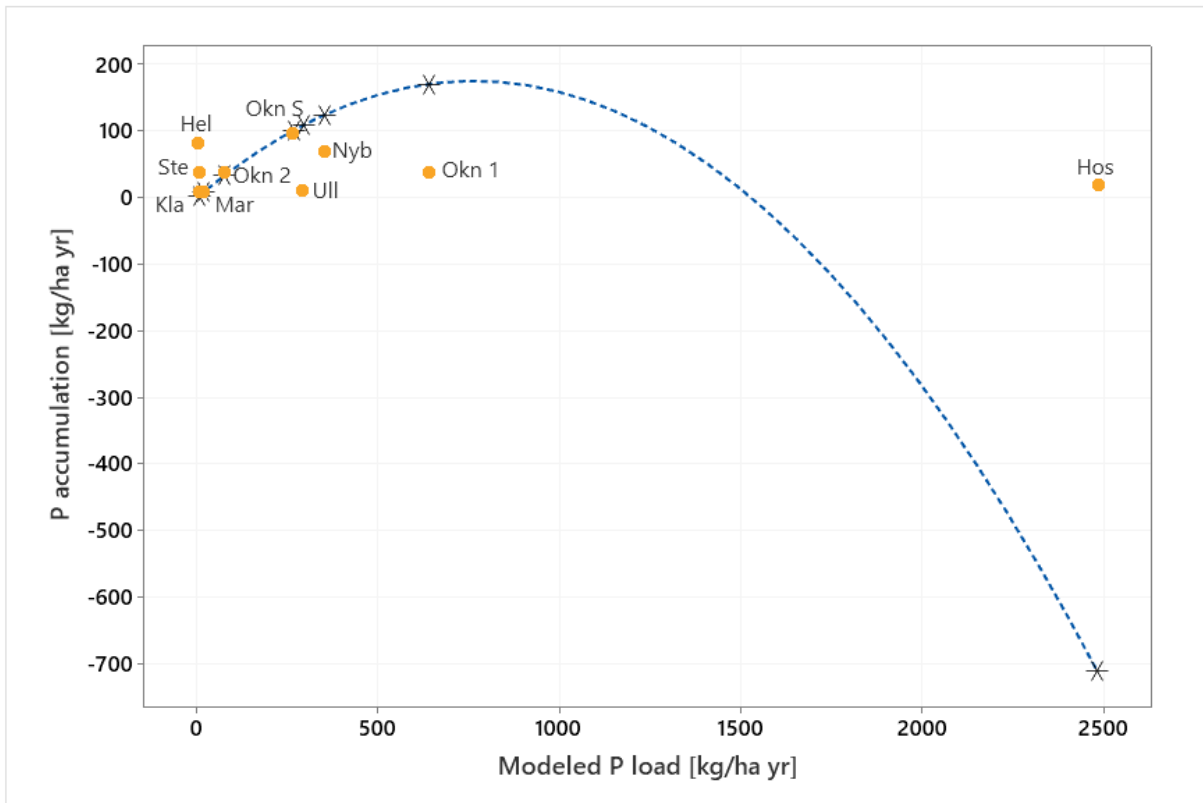


Figure 18. The measured P accumulation (orange) and the potential P retention (star) in relation to the modeled P load. In Hos, a negative potential P retention was estimated based on Weisner's polynomial equation (6) (dashed line).

The observed relationship between modeled long-term  $HL_{LT}$  and total P accumulation in the CWs is presented in Figure 19. There was no statistically significant trend between the two variables (polynomial fit  $R^2 = 13.0\%$ ,  $p = 0.61$ ). The P accumulation measured at the inlets of the CWs was also evaluated in relation to  $HL_{LT}$  (Figure 20), but no correlation could be established (polynomial fit  $R^2 = 11.2\%$ ,  $p = 0.65$ ). However, Okn S, Nyb, and Okn 2 have a significantly higher P accumulation at the inlets compared to the average P accumulation of the CW sections. Based on the accumulation at the inlets, it is distinguished that an  $HL_{LT}$  up to approximately  $210 \text{ m yr}^{-1}$  seems to promote P accumulation.

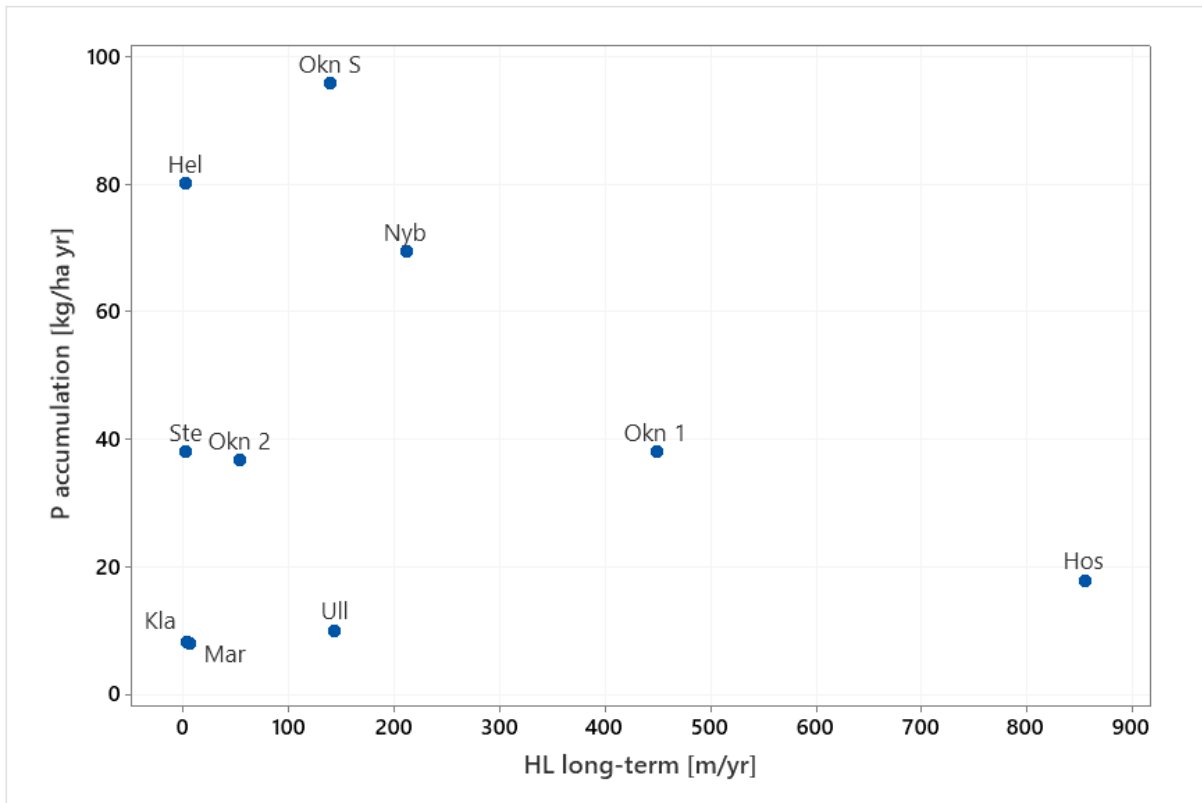


Figure 19. The total P accumulation in relation to the long-term HL.

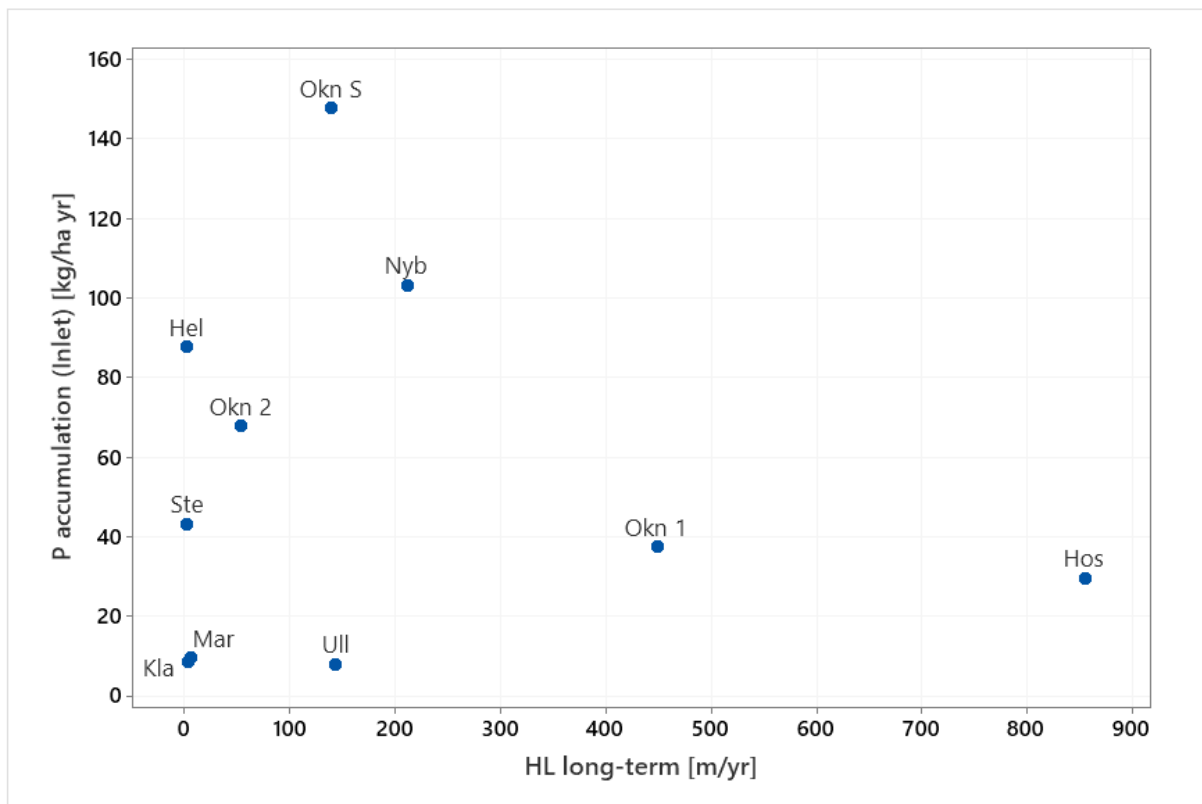


Figure 20. The P accumulation at the inlets of the wetlands in relation to the long-term HL.

The relation between total particle accumulation and long-term  $HL_{LT}$  was also evaluated. Similar trends to the ones seen between the P accumulation and  $HL_{LT}$  could be observed (Figure 21). Excluding Hel, a polynomial trend line gave the best fit to the data. However, no statistical correlation could be established ( $R^2 = 56.2\%$ ,  $p = 0.084$ ). With further exclusion of the CWs with  $HL_{LT} > 210 \text{ m yr}^{-1}$ , a positive linear trend between DW accumulation and  $HL_{LT}$  was observed ( $R^2 = 67.6\%$ ,  $p = 0.023$ , Figure 22).

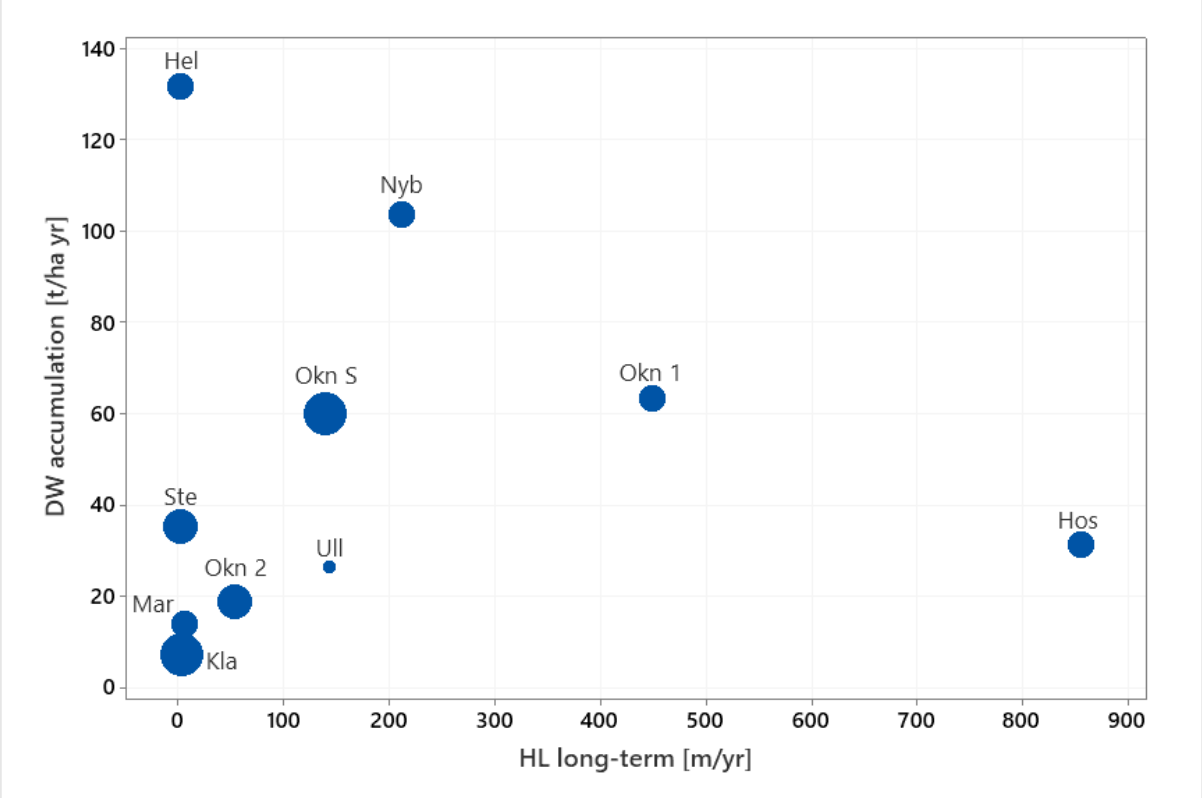


Figure 21. The total particle accumulation in relation to the long-term HL. The size of the circles indicates the P concentration in sediment, where a large circle corresponds to a high concentration.

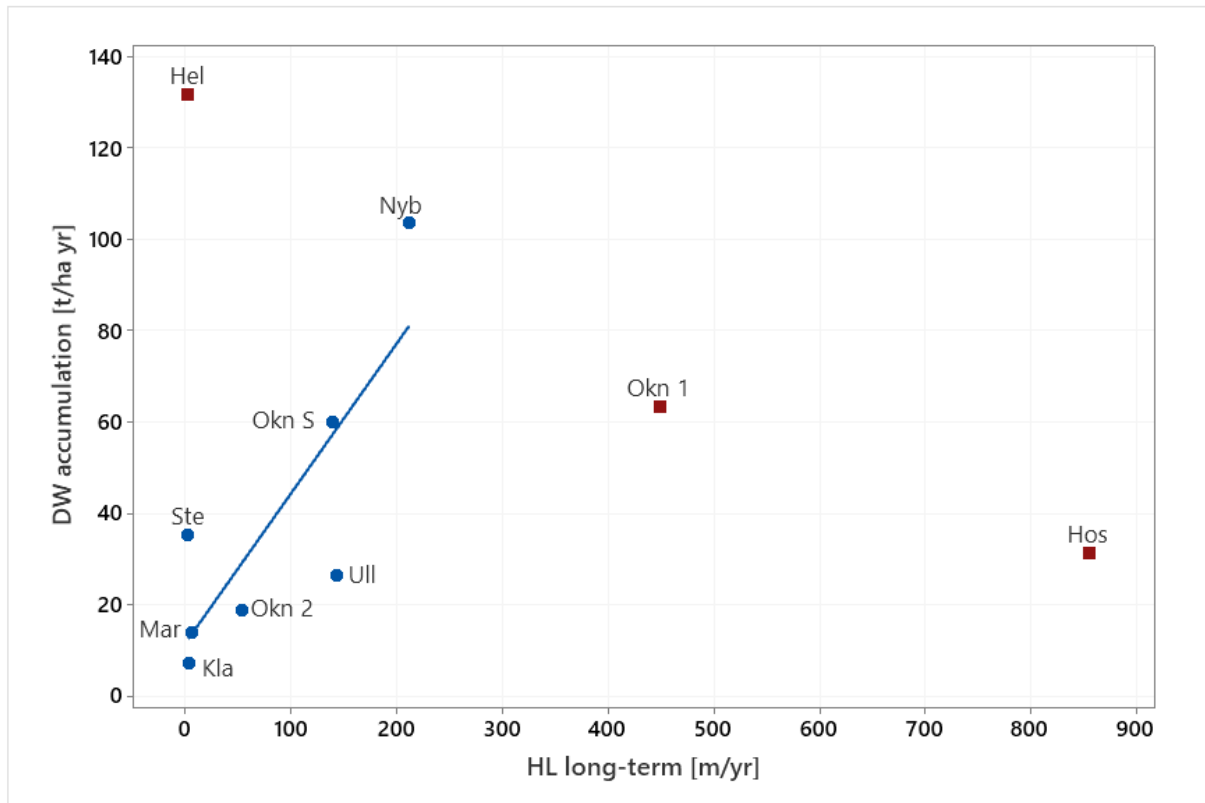


Figure 22. The total particle accumulation in relation to the long-term HL. With Hel, Okn 1, and Hos excluded:  $R^2 = 67.6\%$ ,  $p = 0.023$ .

The erosion risk class had no statistical correlation to either the P accumulation or the DW accumulation (Figure 23 and Figure 24, respectively). However, a slightly negative trend between DW and the erosion risk class could be observed ( $R^2 = 15.0\%$ ,  $p = 0.269$ ). Nyb and Hel located in areas with risk class 3 were found to have the largest particle accumulation. Moreover, Okn 1 and Okn S (risk class 4) had retained more particles than Ste and Kla (risk class 5). At the same time, the other CWs in risk class 3 (Hos, Ull, Mar) had similar particle accumulation as CWs located in areas with lower erosion risk.

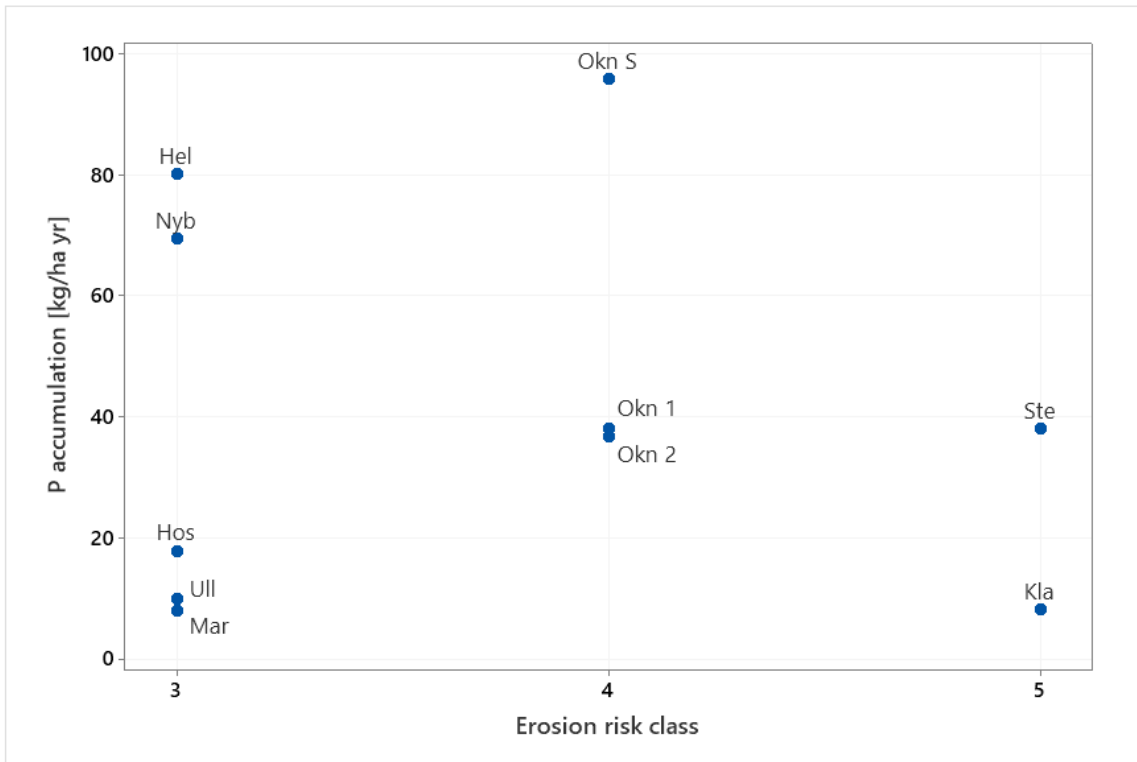


Figure 23. The total P accumulation in relation to the erosion risk class of the CW.

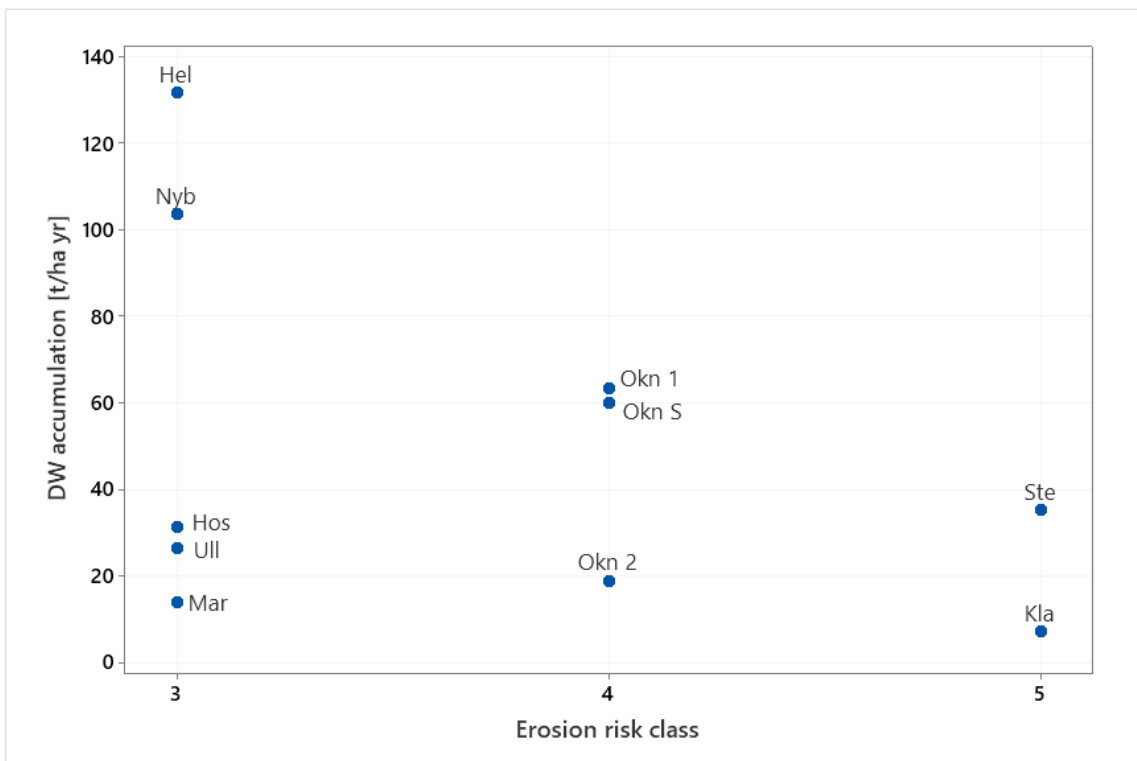


Figure 24. The total particle accumulation in relation to the erosion risk class of the CW.

The total P concentration in sediment was found to have a positive correlation to the erosion risk class of the wetland ( $R^2 = 55.7\%$ ,  $p = 0.013$ , Figure 25). The CWs with the largest expected particle load (risk class 3) had the lowest measured concentrations in sediment, while CWs at less risk of receiving eroded material generally had a higher concentration.

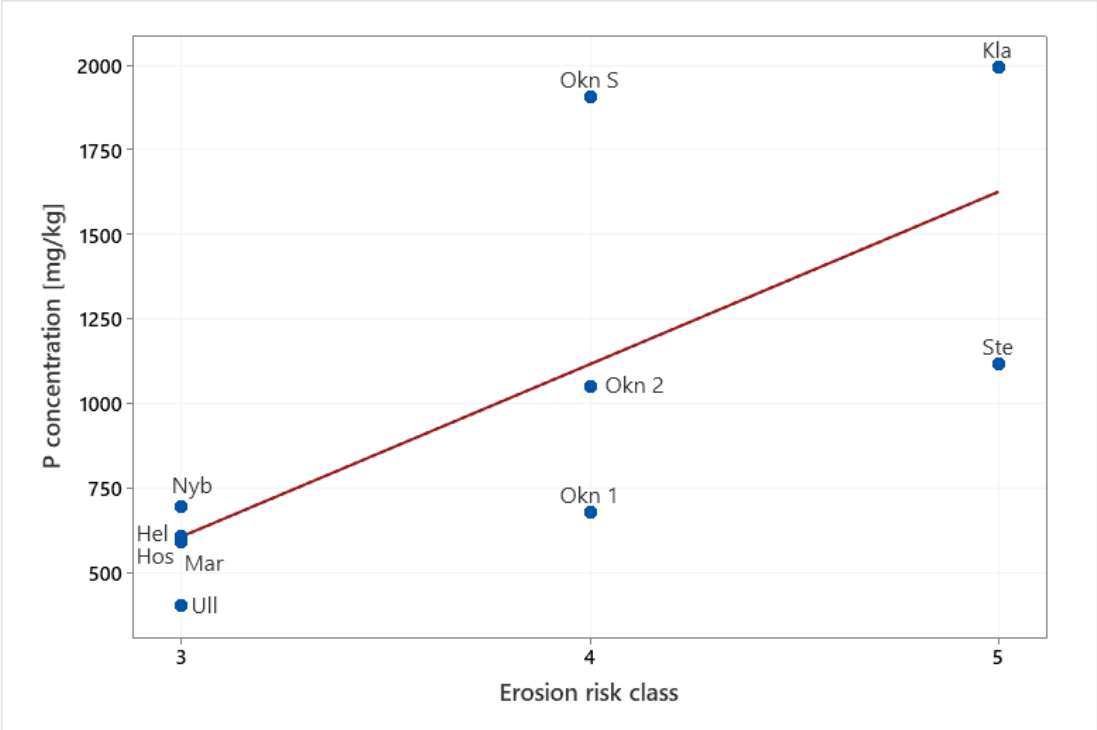


Figure 25. The total P concentration in sediment in relation to the erosion risk class,  $R^2 = 55.7\%$ ,  $p = 0.013$ .

## 5. DISCUSSION

### 5.1. SEDIMENT ACCUMULATION IN THE WETLAND SECTIONS

The examined CWs with different sizes, shapes, and catchment characteristics were shown to have a great variety in sediment accumulation; an average from 0.3 cm yr<sup>-1</sup> to 2.4 cm yr<sup>-1</sup>. The observed accumulation also varied between the CW sections of where the sediment was collected. The water slows down as it enters the wetland, which allows particles in the water to settle to the bottom of the wetland. If a deeper area is constructed at the inlet, this can further promote the sedimentation process (Braskerud 2001a; Jordbruksverket 2004). Therefore, a higher accumulation in the initial areas of the CW can be expected if this is applied. This has been shown in previous studies of P-wetlands, where most particles (50-80% of the total particle accumulation) were retained in the initial areas of the wetland (Braskerud et al. 2000; Geranmayeh et al. 2018). Furthermore, studies have shown how the sediment accumulation decreases with distance from the inlet (Braskerud et al. 2000; Johannesson et al. 2011). Accordingly, the largest sediment accumulation in the P-wetlands was found at the inlet (Hos and Nyb) and the end of the sedimentation basin (Ull) (Figure 8). Four of the seven ponds (Kla, Okn 1, Okn 2, Okn S) also received a larger accumulation layer in the inlet than the outlet, which indicates that they functioned as sediment traps.

No consistent decrease in accumulation was observed in the measured CW sections of the P-wetlands. For instance, the amount of accumulated sediment at the inlet of Hos was also measured at the outlet in the shallow vegetation section (Figure 8). Since no correlation could be established between annual sediment accumulation and water depth in the CWs, this indicates that other factors have a greater influence on the sedimentation patterns taking place in the wetlands. However, it can be seen that the annual sediment accumulation seems to decrease in deep water areas > 1.5 m (Figure 10). This suggests that the settling distance becomes too large to promote particle retention.

The HL is a factor that can have a great impact on the sedimentation rate. This may explain why there is no evident difference in sediment accumulation between the inlet and outlet in Hos. Hos is the smallest of the examined CWs and thus, has an extremely large HL and P load (Table 2). Located in an area relatively prone to erosion (risk class 3) and with high loads, Hos can be expected to have a large inflow of particles. However, the high HL can counteract the sedimentation of the inflowing particles. It is possible that particles did not have time to settle in the initial area, given what could potentially have accumulated due to a high particle load. This may have caused particles to settle further down in the wetland, explaining why no difference was observed between the inlet and outlet.

One other explanation of why the examined P-wetlands are experiencing high accumulation at the outlets could be due to emergent vegetation in the shallow sections. As seen in Figure 8, both Nyb and Ull had the second-highest accumulation at the outlet of the wetland (which for Ull was the same as the accumulation at the inlet). Vegetation in the wetland can reduce both water turbulence and water velocity, as well as promote the formation of aggregates through flocculation (Braskerud 2001b). If the water is slowed down, the detention time in the wetland increases which improves the conditions for particles to have time to settle to the bottom. Furthermore, the shallow section shortens the settling distance for particles which is beneficial

during laminar flows (Braskerud 2003). As the vegetation possibly reduces turbulence, the sediment accumulation may be promoted due to the small water depth in the vegetation section. It is however difficult to determine to which extent this may be beneficial. The vegetation has been shown to prevent resuspension of wetland sediment and decrease the water velocity (Braskerud 2003) but at the same time, a decreased water depth (with fixed wetland width) will also increase the velocity of the water which could increase the risk of resuspension.

In a previous study by Geranmayeh et al. (2018) which included Nyb, the accumulation in wetland sediment was found to not only be represented by inflowing particles, especially regarding newly constructed wetlands. The measurements in Nyb were performed two and three years after the wetland was constructed. The measured particle retention in Nyb indicated that eroded and resuspended material had been transported from the deep to the shallow section (Geranmayeh et al. 2018). It was concluded that particularly recently constructed wetlands are prone to internal erosion and resuspension of materials. Considering that Hos was constructed relatively recently (in 2017), internal bottom erosion and resuspension of accumulated particles may also be an explanation of why the accumulation does not differ between inlet and outlet. It is possible that particles re-deposit and accumulate further down in the wetland. However, measurements of sediment deposition in sediment traps (cylindrical traps which capture sediment and prevent resuspension) should be performed in order to draw any conclusions about whether this is the case or not in Hos wetland.

Considering that the CWs are located in agricultural areas with a large share of clay in the topsoil, aggregates may be formed. The aggregates can then settle as the water passes the vegetation section since aggregates have a higher sedimentation velocity than single clay particles. Then again, vegetation has been shown not to affect the clay particle retention in CWs with high HL ( $HL > 400 \text{ m yr}^{-1}$ ) since this may cause a limitation to the flocculation of clay particles (Braskerud 2001b). Thus, it is unlikely that the vegetation in Hos has promoted the accumulation of aggregates since Hos has an  $HL_{LT}$  of  $850 \text{ m yr}^{-1}$ .

There is a possibility that accumulated sediment consists to some extent of internally generated organic material, such as plant litter, instead of inflowing particles (Johannesson et al. 2015). This was observed by Johannesson et al. (2015) in P-wetlands where the sediment in the shallow vegetation section had higher organic carbon and nitrogen content compared to the deeper section. This suggests that an internal load of organic matter had settled further down in the CWs, rather than particles from inflowing water. The water content of the sediment is a further indicator of this since an increased water content, i.e. less bulk density of the sediment, together with increased OM indicates that the material is internally generated. However, the bulk density decreases as the organic matter increases, but will also vary depending on mineral composition and how the solid particles are packed together (Bauer 1974). When looking at the OM for Hos, Nyb, and Ull, there is no indication that the outlet accumulation would consist of more internally generated material (Table 3). The lowest OM was found in the sediment of Ull's outlet (10%), while the inlet had the most OM (23%). The bulk density did however not vary between the sampling points, which suggests that there is a

possible variation in the mineral composition of settled particles. Hos had the greatest organic matter content at the beginning of the vegetation zone (16%), while the outlet only had 5% OM. The inlet in Hos had the least OM (4%) and a higher density ( $1.4 \text{ g cm}^{-3}$ ), indicating an accumulation of inflowing particles from the catchment. The sediment accumulation at the outlet in Nyb consisted of 7% OM, while the other wetland sections had 6-7% OM in the sediment. Accordingly, the density of the sediment did not differ significantly between the sampling points ( $1.4\text{-}1.5 \text{ g cm}^{-3}$ ).

Three of the ponds (Hel, Mar, Ste) also received more accumulated sediment at the outlet of the wetland than at the inlet. For Hel and Ste, this corresponded to a higher sediment accumulation in the deeper part of the wetland. The inlets of Hel and Ste had a water depth of less than 1 m (0.4-0.5 m), which may not have been sufficient to slow down the water as it enters the wetland, causing particles to settle further down in the wetland where the water depth increased. On the other hand, Hel and Ste are the wetlands with the smallest HL. Considering the fact that other CWs with a shallower initial area of the wetland, together with a larger HL, have more accumulation at the inlet indicates that there is some other factor affecting the accumulation patterns in Hel and Ste. A possible explanation of the accumulation in Hel's outlet can be due to shore erosion (Figure 5). This causes an internal load of particles that accumulate in the wetland, instead of particles transported from the catchment. The sediment cores were also observed to contain a great amount of what appeared to be aggregated clay, possibly originated from the adjacent arable field. It was noticed that the arable land along the west side of Hel was plowed down to the shore in some areas. Consequently, soil particles could have entered the wetland through surface runoff from the shore, and accumulated further down in the wetland.

When sediment cores were sampled in Mar, it was noticed that there was a furrow from the original ditch in the wetland, with greater water depth than areas closer to the shores. Thus, it is likely that a preferential flow path is developed in the formed channel, causing a lower hydraulic efficiency. The residence time in Mar will decrease if flow short-circuiting is occurring, which might explain why particles did not have time to settle in the initial area, and more accumulated sediment was found further down in the wetland. There is also a possibility that internally generated organic material may explain the large accumulation at the outlets of these Hel, Mar, and Ste. However, the results from the sediment analysis suggest that this is not the case (Table 3). Hel does not differ significantly between the sampling points, and Ste has the same organic matter content in the sediment of the inlet and outlet. Mar, on the other hand, had a much higher OM at the inlet than the outlet; 20 and 5%, respectively.

## **5.2. THE PHOSPHORUS AND PARTICLE ACCUMULATION IN WETLAND SEDIMENT**

### **5.2.1. Modeled P load and potential P retention**

The P load was found to be strongly correlated to  $HL_{LT}$  ( $R^2 = 98.7\%$ ,  $p < 0.001$ ), which could be expected since the P load is modeled based on specific runoff data. Hence, the P load increases with an increased HL. Moreover, the potential P retention estimated with Weisner's polynomial equation (6) will increase with increasing P load up to a breaking point, which could be observed in Figure 18. Weisner's equation was a good estimation for four of the

CWs but was shown to highly overestimate the P retention in Nyb, Okn 1, and Ull. The potential P retention in Hel was underestimated compared to the accumulation based on the sampled sediment cores. However, as previously mentioned, this is likely a result of internal erosion of particles with associated P. For Hos, the equation resulted in negative P retention due to the extremely high P load (Table 2). Weisner's equation is however based on measured P loads and retentions at maximum values of 800 and 200 kg ha<sup>-1</sup> yr<sup>-1</sup>, respectively. The modeled P load in Hos is more than three times higher than the measured P load in the study (Weisner et al. 2015), which makes the polynomial equation not applicable for the estimation of P accumulation in Hos.

The potential P retention is likely overestimated since only the positive effects of a high HL will be considered, where a large expected particle load with associated P potentially can lead to a large accumulation. A large HL can reduce the residence time which may be too short for particles to settle. Both Nyb and Okn 1 have a high HL<sub>LT</sub> (211 and 448 m yr<sup>-1</sup>, respectively), which possibly caused the overestimated P retention. However, it is important to point out that the HL is based on average annual streamflow data. Hence, the particle and P accumulation in Nyb were still among the highest of the studied CWs since the water flow that reaches the wetland fluctuates throughout the year, causing conditions more or less beneficial for the particle sedimentation. Okn 1, on the other hand, differs significantly more between the calculated and the measured P retention, which indicates a negative effect of the high HL.

Ull was shown to have among the smallest P accumulations compared to the other CWs although the HL and P load is high (Table 4). The overestimated P retention in Ull may be explained by the low P concentration in the wetland sediment. Since modeled P load is also based on land use and soil-specific export coefficients, Ull's catchment may contain less P than what is usually found in such types of land use and soils. The land use in Ull's catchment is relatively similar to many of the other CWs, where Ull has one of the largest proportions of arable land (Appendix A.2.). However, it is also possible that the P concentration in sediment was low at the time of the sampling. It was still an ice cover on Ull's water surface when the sediment cores were collected. A lower water flow and reduced mixing of the water mass can lead to altered redox conditions. Since it is common for P to bind to Fe-hydroxide complexes in the sediment (Ulén 2005), the Fe-P complex formation may have ceased as the oxygen content decreased. Consequently, P can be released into the water which would explain why a low P concentration was measured in the wetland sediment. This is further strengthened by the observation of the sediment cores. Orange elements of Fe-precipitate were noticed in Ull, which indicates that Fe is present in the wetland and potentially can bind (and release) a great amount of P (Table 3). It would be of interest to re-sample the sediment in Ull to see if the P concentration and, consequently, the P accumulation is higher due to changed redox conditions when there is no ice present.

### **5.2.2. Particle retention and clay content in the topsoil influencing P accumulation**

If the sedimentation process of particles is not promoted in the wetland, the particle accumulation can be expected to be small. If fewer particles are retained in the wetland, less P will be retained since a significant part of the P is presumably attached to fine-textured

particles. Johannesson et al. (2015) found a strong correlation between P retention and particle retention. Similarly, the P accumulation in the CWs in this study was found to be positively correlated to the particle accumulation ( $R^2 = 61.76\%$ ,  $p = 0.007$ , Figure 11). The total P accumulation varied between 8 and 96 kg ha<sup>-1</sup> yr<sup>-1</sup> (Table 4). Other Swedish wetlands have shown similar variations with P accumulations between 11 and 175 kg ha<sup>-1</sup> yr<sup>-1</sup> (Johannesson et al. 2015). One significant difference is however how the P accumulation relates to the clay content of the topsoil.

The CWs included in this study are all situated in areas with a high clay content of the agricultural topsoil (27-37%). It can therefore be expected that the CWs have a potentially high accumulation of particles and associated P since arable fields with clay soils have shown to have among the highest P-losses (Johannesson et al. 2015). Accordingly, the total particle and P accumulation was positively correlated to the clay content of the topsoil (Figure 16). Hence, increased clay content of the topsoil in the catchment generally increased the particle and associated P retention. On the contrary from the results of this study, a negative correlation between particle and P accumulation and the clay content was found by Johannesson et al. (2015), where the least amount of retained P corresponded to a clay content of 33% (Wig wetland), and the largest accumulation to 19% clay (Gen wetland). This suggests that the sedimentation process was promoted in most CWs in this study even though the inflowing particles potentially consisted of a large proportion of clay particles. However, a particle size distribution analysis of the sediment would be necessary to draw any conclusions about to which extent clay particles were retained in the wetlands.

The P concentration will also influence the amount of P that is retained in the wetland. The largest P retention was found in Okn S although fewer particles were retained compared to Okn 1, Nyb, and Hel (Figure 11). However, the P concentration in Okn S was approximately three times higher, which resulted in a larger P accumulation. In this study, P concentrations varied between 400 and 2000 mg kg<sup>-1</sup>. Johannesson et al. (2015) found that the average P concentrations varied between 738 and 2800 mg kg<sup>-1</sup>. Hence, the high concentrations in Okn S and Kla (1900 and 2000 mg kg<sup>-1</sup>, respectively) are not considered to be abnormally high. The one that stands out the most is the P concentration in Ull (400 mg kg<sup>-1</sup>). As discussed before, P has likely been released into the water, resulting in a lower P concentration in the sediment. In addition, the CWs with the largest expected particle load (risk class 3) had the lowest measured concentrations in sediment, while CWs at less risk of receiving eroded material generally had a higher concentration (Figure 25). This further emphasizes that a particle size distribution analysis of the sediment should be performed to see how clay particles are retained in the wetlands since they potentially can bind a great amount of P.

The proportion of agricultural land within each catchment did not correlate with either the particle accumulation or the P accumulation. However, since all CWs have a significant proportion of agricultural land in the catchment area and a high potential nutrient load, other factors are likely to have a greater impact on how particles and associated P are retained in the wetland.

### 5.2.1. Design, relative size to catchment, and erosion risk influencing total P and DW accumulation

It could be expected for CWs with a large surface area to have retained more particles and associated P since particle retention has shown to increase with increased surface area (Braskerud 2001a; Sveistrup et al. 2008). However, no such correlation was observed in the studied CWs. Nor did the particle and P accumulation show any correlation to the water depth in the wetland. It could however be observed that the P retention was low in deep water areas (> 1.5 m), while water depths up to approximately 1 m resulted in a large variety of accumulated P. This suggests that the water depth should be limited to approximately 1 m to avoid too large particle settling distances which may inhibit the particle and associated P retention.

In this study, no correlation between total P accumulation and  $A_W:A_C$  could be observed (Figure 14). Nor did the  $A_W:A_C$  ratio show any correlation to the total particle accumulation or annual sediment accumulation. Some expected accumulation patterns could however be distinguished. For instance, K1a with a large  $A_W:A_C$  ratio of 4.9% had a low DW accumulation ( $7 \text{ t ha}^{-1} \text{ yr}^{-1}$ ) and total P accumulation ( $8 \text{ kg ha}^{-1} \text{ yr}^{-1}$ , Figure 14). This can be explained by a low inflow of water to the wetland relative to its area. Hence, the particle load can be expected to be low which results in a low accumulation of particles and associated P. This is supported by the fact that K1a is located in an area less prone to erosion (erosion risk class 5). Different from K1a, Ste had a larger P and DW accumulation ( $38 \text{ kg ha}^{-1} \text{ yr}^{-1}$  and  $35 \text{ t ha}^{-1} \text{ yr}^{-1}$ ). Ste is located within the same area of erosion risk class 5 and has the largest  $A_W:A_C$  ratio of all CWs (7%). Accordingly, the HL in Ste is small ( $2.45 \text{ m yr}^{-1}$ ), since the correlation between HL and  $A_W:A_C$  is commonly found to be negative (Kynkäänniemi 2014). Ste could therefore be expected to obtain a low particle accumulation similar to K1a, but instead has five times as many retained particles and more than four times as much P accumulated. One factor that may influence the increased accumulation is the type of water inflow. The water enters Ste through an open ditch while K1a has drainage pipes at both inlets. Bank erosion of the open ditch may contribute to an increased particle transport, together with surface runoff from the arable field to the ditch in the event of heavy rainfall.

The smaller CWs with similar  $A_W:A_C$  ratios were shown to have a substantial difference in P accumulation (Figure 14). This was also observed by Braskerud (2001a), who explained it by differences in catchment factors, such as soil type, climate, and farm management practice. Although this may be true, the CWs in this study have relatively similar soil textures in their catchments and are located within the same geographical area. For instance, Nyb is located in an area more prone to erosion (erosion class 3) and had the largest annual sediment accumulation and DW accumulation of the smaller CWs. At the same time, other small CWs (Okn 1, Okn S) in areas with less erosion risk (class 4) had more accumulation than CWs in risk class 3 (Ull and Hos). Thus, no correlation could be established between the erosion risk class and the particle and P accumulation, even though DW was slightly negatively related to the erosion risk class (Figure 23). This suggests that a high expected particle load does not necessarily mean high particle retention and that other factors influence how well the particles are retained in the wetland. For instance, a shorter residence time in the CWs with higher HL might counteract particle retention.

### 5.2.3. Hydraulic load and efficiency influencing total P and DW accumulation

Looking at the influence of HL on the total particle and P accumulation, no correlation could be established (Figure 19, Figure 21). However, an HL up to approximately  $210 \text{ m yr}^{-1}$  seemed to have a positive influence on the particle and P accumulation, resulting in a relatively large amount of accumulated P and particles. This corresponded to CWs with  $A_w:A_c$  ratios larger than 0.1%. For  $HL > 210 \text{ m yr}^{-1}$ , the accumulation decreased. This possible turning point is more noticeable when looking at the P accumulation at the inlets (Figure 20). It should however be emphasized that a high HL, causing a high expected particle load, does not necessarily lead to a high P accumulation even if the retention of particles is large in the wetland. If the inflowing water and particles have a low P concentration, the total P accumulation might be low even if the particle sedimentation is promoted. For instance, Ull has a relatively high  $HL_{LT}$  ( $143 \text{ m yr}^{-1}$ ) but the lowest measured P concentration in the sediment of all CWs. Consequently, the P accumulation is low due to the low concentration (Figure 19, Figure 20). Hel has a higher P concentration ( $600 \text{ mg kg}^{-1}$ ) together with the largest amount of settled particles ( $DW 130 \text{ t ha}^{-1} \text{ yr}^{-1}$ ). As a result of large particle deposition, a great amount of P is retained in the wetland. It should however be noted that the total particle deposition in Hel is unexpectedly high since the modeled  $HL_{LT}$  is the smallest of all CWs. As previously mentioned, this might be a result of internal erosion rather than transport and deposition of particles that originated only from the catchment area.

Similar accumulation patterns of particles and P in relation to HL have been observed in previous studies. Kynkäänniemi (2014) observed that the wetlands Bölarp and Wiggeby with HL of  $300$  and  $400 \text{ m yr}^{-1}$  resulted in low particle and associated P accumulation (which corresponded to wetlands with  $A_w:A_c$  ratios smaller than 0.1%). The other wetlands ( $A_w:A_c > 0.1\%$ ) had a strong positive correlation between particle and associated P retention and HL ( $HL < 250 \text{ m yr}^{-1}$ ). Johannesson et al. (2015) also observed the lowest particle retention in the Wiggeby wetland although it was designed to obtain a good hydraulic efficiency (L:W 7). Johannesson et al. (2015) concluded that there may be a breakpoint of HL where the retention of particle and associated P is inhibited even if the L:W is high. Based on the observations in this study and the results of previous studies, it is likely that the turning point for the HL is in the range between  $200$  and  $300 \text{ m yr}^{-1}$  for wetlands with high L:W ratios. More specifically, an HL up to  $210 \text{ m yr}^{-1}$  ( $A_w:A_c > 0.1\%$ ) will likely have a positive influence on the particle and P accumulation in the wetland. However, it is impossible to determine an optimal HL for P accumulation based on such few observations. It would be of interest to include more wetlands with an HL in the range between  $200$  and  $300 \text{ m yr}^{-1}$  to estimate a more precise turning point.

Considering the fact that the small CWs Hos and Okn 1 ( $A_w:A_c$  0.02 and 0.04%) with  $HL > 210 \text{ m yr}^{-1}$  have catchments with high clay content in the topsoil ( $> 30\%$ ), it is likely that the water that reaches the CWs contains a large proportion of fine particles. As the HL increases, the residence time decreases, which may have been too short for smaller particles to have time to settle in the wetlands. Moreover, the decreased residence time as a result of high flow seems to outweigh the positive influence of good hydraulic efficiency in the wetland, i.e. a high L:W ratio. Previous studies have shown a positive correlation between L:W ratio and

particle and P retention (Kynkäänniemi 2014; Johannesson et al. 2015). However, no correlation between P accumulation and L:W could be demonstrated for the CWs included in this study. Regarding the particle accumulation, L:W was only positively related to the DW when the CWs with extremely large and small particle accumulation were excluded from the analysis (Figure 13). However, all of the studied CWs have a potentially high hydraulic efficiency due to a long and narrow shape, which may explain why the L:W did not have a strong influence on the particle and P accumulation. As mentioned above, factors such as HL may outweigh the positive influence of a high L:W. For instance, Okn S and Ste had both higher particle accumulation than Hos, even if a better hydraulic efficiency could be expected in Hos due to a higher L:W ratio (Figure 13). This further emphasizes the importance of sufficient residence time in the wetland for high particle retention to occur.

### **5.3. METHOD UNCERTAINTIES**

#### **5.3.1. Sediment sampling and measurement**

For most wetlands, two cores were collected in each CW section where the additional sediment core was analyzed regarding particle size distribution (which is not included in the scope of this study). However, it was noted that some cores differed significantly in how much sediment had accumulated, even though they were sampled at the same section in the wetland. A more precise estimate of particle and associated P accumulation could have been obtained with more sampling points. For instance, the sediment depth could have been evaluated in several points along a transect of each CW section.

The sediment sampling was performed on one occasion in each wetland in March 2021. Consequently, seasonal variations in, for example, water depth were not taken into account. However, the results from the fieldwork are considered accurate enough to detect sedimentation patterns and correlations between the accumulation and wetland design and catchment factors.

#### **5.3.2. Software and statistical analysis**

The cartography software ArcMap 10.7.1 was used to calculate wetland area, length, and average width. Orthophotos with 0.25 m/pixel resolution were used which have an estimated average error of 0.3 m (Lantmäteriet 2020). The average width was based on measurements of the wetland width every twenty meters, which was considered to be a good estimate for the calculations of the L:W ratio. Moreover, the land use and proportion of soil particle size distribution within the catchment were calculated using ArcMap. The raster had a resolution of 10×10 m and 50×50 m, respectively, which can be considered to give sufficiently good estimates for the large catchment areas. However, it can always be a good idea to conduct a random sampling in the catchment area to see that the calculated soil texture within the catchment corresponds to the sampling results.

The results are based on a low observation number ( $n = 10$ ), which may not be adequate to provide a precise estimate of the strength of the relationships. Further statistical analyses including more CWs would be optimal to estimate potential correlations with relevant factors. However, the results of this study together with a comparison with previous studies can still be considered as a good indication of how wetland design and catchment factors affect the particle and P accumulation.

### **5.3.3. Modeled hydraulic load**

The catchment areas are based on elevation data where tile drainage systems of arable land were not considered in the catchment estimation. This may have caused an overestimation of HL since there is a possibility that some areas might be included in the CW catchment that does not drain into the wetland. Moreover, downscaling hydrological data from large river basins may not result in an accurate estimation of HL in smaller catchments. In this study, HL was calculated based on modeled flows computed with SMHI's S-HYPE model. Johannesson et al. (2015) used similar hydrological data of large river basins to estimate HL. However, the modeled HL values were found to differ from the measured HL with 11-56%. A similar variation may be found if flow measurement would be performed in the CWs included in this study. However, modeled HL is easily accessible and can give a good first indication of how it is related to sediment accumulation in wetlands.

## 6. CONCLUSIONS

The results of the study showed that the total P accumulation was positively correlated to particle accumulation. The P accumulation in the studied wetlands varied between 8 and 96 kg ha<sup>-1</sup> yr<sup>-1</sup> and the total particle accumulation was 7-130 t ha<sup>-1</sup> yr<sup>-1</sup>.

The wetland design factors had no significant influence on the particle and P accumulation. The CW area and water depth were not correlated to the amount of accumulated P, but greater water depths (> 1.5 m) seemed to inhibit the particle and associated P retention. This suggests that the water depth should be limited to approximately 1 m to avoid too large particle settling distances. No correlation between P accumulation and L:W could be observed. However, all of the studied CWs have a potentially high hydraulic efficiency due to a long and narrow shape, which may explain why the L:W did not show a strong influence on the particle and P accumulation.

The proportion of agricultural land within each catchment did not show any correlation to the P accumulation. The clay content in the topsoil was however positively correlated to both particle and P accumulation. This suggests that the sedimentation process was promoted in most wetlands even though the inflowing particles potentially consisted of a large proportion of clay particles. However, further analysis of the particle size distribution in sediment is necessary to draw any conclusions about to which extent clay particles were retained in the wetlands.

No correlation could be established between the erosion risk class and the particle and P accumulation. The P concentration in sediment did however show a correlation to the erosion risk class. Wetlands with the largest expected particle load had the lowest concentrations in sediment, which further emphasizes that a particle size distribution analysis of the sediment should be performed to evaluate the accumulation of clay particles.

A high HL (450 and 850 m yr<sup>-1</sup>) was shown to counteract the particle and P retention, which corresponded to CWs smaller than 0.1% of the catchment area. No correlation could be established between HL and the P accumulation, but an HL up to approximately 210 m yr<sup>-1</sup> will likely have a positive influence on the particle and P accumulation. This suggests that CWs should be larger than 0.1% of the catchment area to retain P. However, it was not possible to determine an optimal HL to promote P accumulation based on such few observations. The potential breakpoint of HL where the retention of particle and associated P is inhibited is likely in the range between HL 200 and 300 m yr<sup>-1</sup>. However, it would be necessary to include more CWs with an HL in this range to estimate a more precise turning point.

## REFERENCES

- Archfield, S.A. & Vogel, R.M. (2010). Map correlation method: Selection of a reference streamgauge to estimate daily streamflow at ungauged catchments. *Water Resources Research*, 46 (10). <https://doi.org/10.1029/2009WR008481>
- Aronsson, H., Berglund, K., Djodjic, F., Etana, A., Geranmayeh, P., Johnsson, H. & Wesström, I. (2019). *Effekter av åtgärder mot fosforförluster från jordbruksmark och åtgärdsutrymme*. (Ekohydrologi, 160). Uppsala: Sveriges lantbruksuniversitet.
- Bauer, A. (1974). *Influence of soil organic matter on bulk density and available water capacity of soils*. (Farm Research). North Dakota State University of Agriculture and Applied Science.
- Blomqvist, S. & Rydin, E. (2009). *Hur fosforbindningen i Östersjöns bottensediment kan förstärkas*. (5914). Stockholm: Naturvårdsverket.
- Braskerud, B.C. (2001a). *Sedimentation in small constructed wetlands: retention of particles, phosphorus and nitrogen in streams from arable watersheds*. (Ph.D. Thesis). Agricultural University of Norway, Department of Soil and Water Sciences.
- Braskerud, B.C. (2001b). The Influence of Vegetation on Sedimentation and Resuspension of Soil Particles in Small Constructed Wetlands. *Journal of Environmental Quality*, 30 (4), 1447–1457. <https://doi.org/10.2134/jeq2001.3041447x>
- Braskerud, B.C. (2003). Clay particle retention in small constructed wetlands. *Water Research*, 37 (16), 3793–3802. [https://doi.org/10.1016/S0043-1354\(02\)00484-0](https://doi.org/10.1016/S0043-1354(02)00484-0)
- Braskerud, B.C., Lundekvam, H. & Krogstad, T. (2000). The Impact of Hydraulic Load and Aggregation on Sedimentation of Soil Particles in Small Constructed Wetlands. *Journal of Environmental Quality*, 29 (6), 2013–2020. <https://doi.org/10.2134/jeq2000.00472425002900060039x>
- Britannica (2016). Stokes's law. *Encyclopedia Britannica*. <https://www.britannica.com/science/Stokess-law> [2021-02-22]
- Djodjic, F. (2021). Shapefiles of wetlands and calculated catchment areas [Unpublished data]. The Swedish University of Agricultural Sciences.
- Djodjic, F., Geranmayeh, P. & Markensten, H. (2020). Optimizing placement of constructed wetlands at landscape scale in order to reduce phosphorus losses. *Ambio*, 49 (11), 1797–1807. <https://doi.org/10.1007/s13280-020-01349-1>
- Djodjic, F. & Markensten, H. (2019). From single fields to river basins: Identification of critical source areas for erosion and phosphorus losses at high resolution. *Ambio*, 48 (10), 1129–1142. <https://doi.org/10.1007/s13280-018-1134-8>
- Fennessy, M.S., Brueske, C.C. & Mitsch, W.J. (1994). Sediment deposition patterns in restored freshwater wetlands using sediment traps. *Ecological Engineering*, 3 (4), 409–428. [https://doi.org/10.1016/0925-8574\(94\)00010-7](https://doi.org/10.1016/0925-8574(94)00010-7)
- Ferguson, A. (2019). *Size optimization of constructed wetlands for phosphorus retention in agricultural areas*. Uppsala: SLU, Institutionen för mark och miljö. <http://stud.epsilon.slu.se/14739/> [2021-03-17]
- Geranmayeh, P., Johannesson, K.M., Ulén, B. & Tonderski, K.S. (2018). Particle deposition, resuspension and phosphorus accumulation in small constructed wetlands. *Ambio*, 47 (S1), 134–145. <https://doi.org/10.1007/s13280-017-0992-9>
- Hassby, O., Björling, E., Narvelo, W., Bengtsson, F., Nihlén, C. & Widarsson, L.-E. (2015). *Anlagda våtmarker - Våtmarker, tvåstegsdiken och dagvattendammar i Helsingborgs stad*. Helsingborg: Stadsbyggnadsförvaltningen.
- HELCOM (2019). *Inputs of nutrients (nitrogen and phosphorus) to the sub-basins (2017)*. [https://helcom.fi/wp-content/uploads/2019/08/HELCOM-core-indicator-on-inputs-of-nutrients-for-period-1995-2017\\_final.pdf](https://helcom.fi/wp-content/uploads/2019/08/HELCOM-core-indicator-on-inputs-of-nutrients-for-period-1995-2017_final.pdf) [2021-04-16]
- HELCOM (2020). *Inputs of nutrients (nitrogen and phosphorus) to the subbasins (2018)*

- Hellgren, S. (2021). Flow direction raster and flow accumulation raster calculated based on elevation data [Unpublished data]. The Swedish University of Agricultural Sciences.
- Johannesson, K.M., Andersson, J.L. & Tonderski, K.S. (2011). Efficiency of a constructed wetland for retention of sediment-associated phosphorus. *Hydrobiologia*, 674 (1), 179–190. <https://doi.org/10.1007/s10750-011-0728-y>
- Johannesson, K.M., Kynkäänniemi, P., Ulén, B., Weisner, S.E.B. & Tonderski, K.S. (2015). Phosphorus and particle retention in constructed wetlands—A catchment comparison. *Ecological Engineering*, 80, 20–31. <https://doi.org/10.1016/j.ecoleng.2014.08.014>
- Jordbruksverket (2004). *Kvalitetskriterier för våtmarker i odlingslandskapet – kriterier för rening av växtnäring med beaktande av biologisk mångfald och kulturmiljö*. (2004:2). Jönköping: Jordbruksverket.
- Jordbruksverket (2010). *Dammar som samlar fosfor*. [https://www2.jordbruksverket.se/webdav/files/SJV/trycksaker/Pdf\\_jo/jo10\\_11.pdf](https://www2.jordbruksverket.se/webdav/files/SJV/trycksaker/Pdf_jo/jo10_11.pdf)
- Kroetsch, D. & Wang, C. (2008). *Particle Size Distribution*. (Carter, M. R. & Gregorich, E. G., eds.) 2nd ed. [Pinawa, Manitoba] : Boca Raton, FL: Canadian Society of Soil Science ; CRC Press. (Soil sampling and methods of analysis)
- Kynkäänniemi, P. (2014). *Small wetlands designed for phosphorus retention in Swedish agricultural areas efficiency variations during the first years after construction*. Uppsala: Dept. of Soil and Environment, Swedish University of Agricultural Sciences. <http://urn.kb.se/resolve?urn=urn:nbn:se:slu:epsilon-e-2080> [2021-02-16]
- Lannergård, E.E., Agstam-Norlin, O., Huser, B.J., Sandström, S., Rakovic, J. & Futter, M.N. (2020). New Insights Into Legacy Phosphorus From Fractionation of Streambed Sediment. *Journal of Geophysical Research: Biogeosciences*, 125 (9), e2020JG005763. <https://doi.org/10.1029/2020JG005763>
- Lantmäteriet (2020). *Produktbeskrivning - Ortofoto*. <https://www.lantmateriet.se/globalassets/kartor-och-geografisk-information/flyg--och-satellitbilder/ortofoto.pdf>
- Naturvårdsverket (2020). *Ladda ned Nationella Marktäckedata*. Naturvårdsverket. [text]. <https://www.naturvardsverket.se/Sa-mar-miljon/Kartor/Nationella-Marktaeckedata-NMD/Ladda-ned/> [2021-03-11]
- Naturvårdsverket (2020b). *Miljömålen: Årlig uppföljning av Sveriges nationella miljömål 2020 – Med fokus på statliga insatser*. (6919). Stockholm.
- Naturvårdsverket (2020c). *Nationella marktäckedata 2018 basskikt*. (Utgåva 2.2). Stockholm. [https://gpt.vic-metria.nu/data/land/NMD/NMD\\_Produktbeskrivning\\_NMD2018Basskikt\\_v2\\_2.pdf](https://gpt.vic-metria.nu/data/land/NMD/NMD_Produktbeskrivning_NMD2018Basskikt_v2_2.pdf) [2021-03-10]
- Nimmo, J.R. (2013). Aggregation: Physical Aspects. *Reference Module in Earth Systems and Environmental Sciences*. Elsevier. <https://doi.org/10.1016/B978-0-12-409548-9.05087-9>
- Persson, J., Somes, N.L.G. & Wong, T.H.F. (1999). Hydraulics efficiency of constructed wetlands and ponds. *Water Science and Technology*, 40 (3), 291–300. [https://doi.org/10.1016/S0273-1223\(99\)00448-5](https://doi.org/10.1016/S0273-1223(99)00448-5)
- SMHI (2020-04-23). *S-HYPE: HYPE-modell för hela Sverige*. <https://www.smhi.se/forskning/forskningsenheter/hydrologisk-forskning/s-hype-hype-modell-for-hela-sverige-1.560> [2021-06-21]
- SMHI (2021). *Vattenwebb - Modelldata per område*. <http://vattenwebb.smhi.se/modelarea/> [2021-02-25]
- Söderström, M. & Piikki, K. (2016). *Digitala åkermarkskartan – detaljerad kartering av textur i åkermarkens matjord*. (37). Skara: Institutionen för mark och miljö, Precisionsodling och Pedometri.

- Sveistrup, T.E., Marcelino, V. & Braskerud, B.C. (2008). Aggregates explain the high clay retention of small constructed wetlands: a micromorphological study. *Boreal Environment Research*, 13 (3), 275–284
- Swedish Environmental Protection Agency (n.d.). *National Land Cover Database*. Swedish Environmental Protection Agency. [text]. <http://www.swedishepa.se/State-of-the-environment/Maps-and-map-services/National-Land-Cover-Database/> [2021-03-11]
- Ulén, B. (2005). *Fosforförluster från mark till vatten: identifikation av kritiska källor och möjliga motåtgärder*. (5507). Stockholm: Naturvårdsverket.
- Weisner, S., Johannesson, K. & Tonderski, K. (2015). *Näringsavskiljning i anlagda våtmarker i jordbruket - Analys av mätresultat och effekter av landsbygdsprogrammet*. (Rapport 2015:7). Jönköping: Jordbruksverket. [https://www2.jordbruksverket.se/download/18.704fc84714d2baac7efc9b0c/1431091028248/ra15\\_7.pdf](https://www2.jordbruksverket.se/download/18.704fc84714d2baac7efc9b0c/1431091028248/ra15_7.pdf)
- Wörman, A. & Kronnäs, V. (2005). Effect of pond shape and vegetation heterogeneity on flow and treatment performance of constructed wetlands. *Journal of Hydrology*, 301 (1), 123–138. <https://doi.org/10.1016/j.jhydrol.2004.06.038>

## APPENDIX

### A.1. PARTICLE SIZE DISTRIBUTION OF THE TOPSOIL

Table 5. Calculated particle size distribution in the topsoil of agricultural areas within CW catchments. The soil texture is determined based on the Digital Arable Soil Map of Sweden (DSMS). The DSMS area within each catchment is based on agricultural land in 2013, registered by the Swedish Board of Agriculture. For comparison, the area of registered agricultural land in 2018 is presented (Jbv block 2018).

CW	Clay [%]	Silt [%]	Sand [%]	DSMS area [ha]	Jbv block 2018 [ha]
Okn	30	47	23	100	104
Okn 1	30	47	23	97	100
Okn 2	30	49	21	3	4
Hos	32	47	21	72	75
Nyb	36	46	18	31	33
Okn S	37	42	21	27	29
Ull	34	47	20	68	65
Mar	33	49	19	31	31
Kla	27	45	28	69	68
Hel	36	48	16	32	31
Ste	29	46	25	10	11

## A.2. LAND USE DISTRIBUTION IN THE CATCHMENT AREA

The land use distribution within each catchment is presented in Table 6. The land cover categories that dominate most catchments are arable land, pasture, and forest, based on The National Land Cover Database.

*Table 6. Determined land use distribution within CW catchments, based on data from The National Land Cover Database. Fields with “-” indicate that there is no, or too small to be detected, corresponding land fraction within the catchment area.*

CW	Land use distribution [%]							
	Arable land	Pasture	Forest	Temporary non-forest	Exploited land	Open land	Open wetland	Water
Okn	42	9	39	3	4	2	<1	<1
Okn 1	43	8	40	3	4	2	<1	-
Okn 2	15	57	13	<1	-	<1	1	13
Hos	60	4	23	3	4	6	<1	-
Nyb	38	<1	49	3	4	5	-	<1
Okn S	43	15	23	2	9	9	-	-
Ull	49	<1	37	2	4	6	<1	<1
Mar	63	-	23	4	3	4	-	3
Kla	49	<1	30	3	5	8	<1	5
Hel	30	22	28	9	1	4	-	6
Ste	41	8	26	3	5	11	6	-

**A.3. MAPS OF WETLAND CATCHMENT AREAS AND EROSION RISK CLASSES**

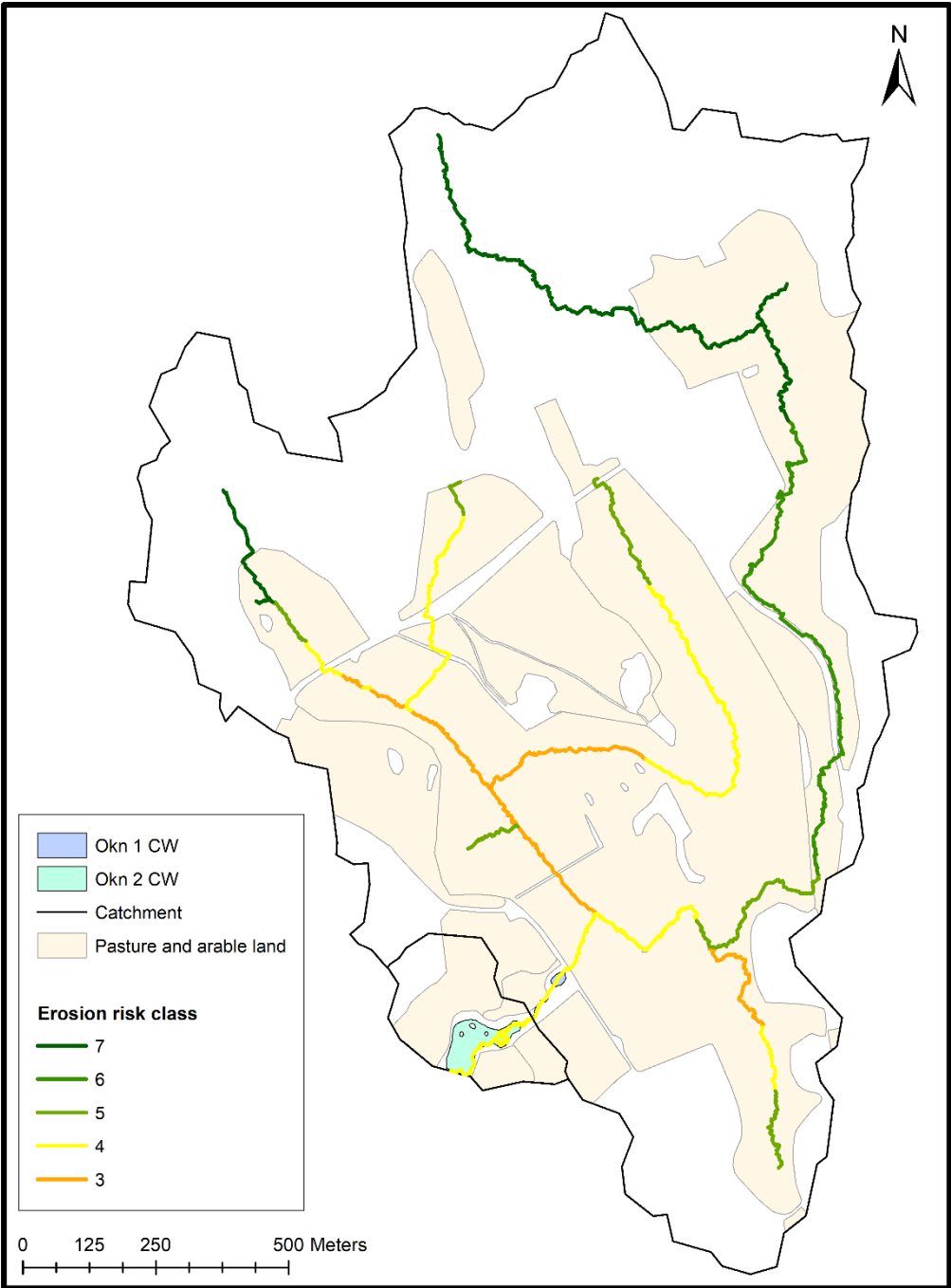


*Figure 26. A map of the connected CWs Okn 1 and 2 and their corresponding catchment areas. Beige markings display pasture and arable land areas. Erosion risk classes vary from 3 to 7 within the catchments, where risk class 7 implies the lowest expected particle load. The dominating erosion risk class closest to the CWs is class 4.*

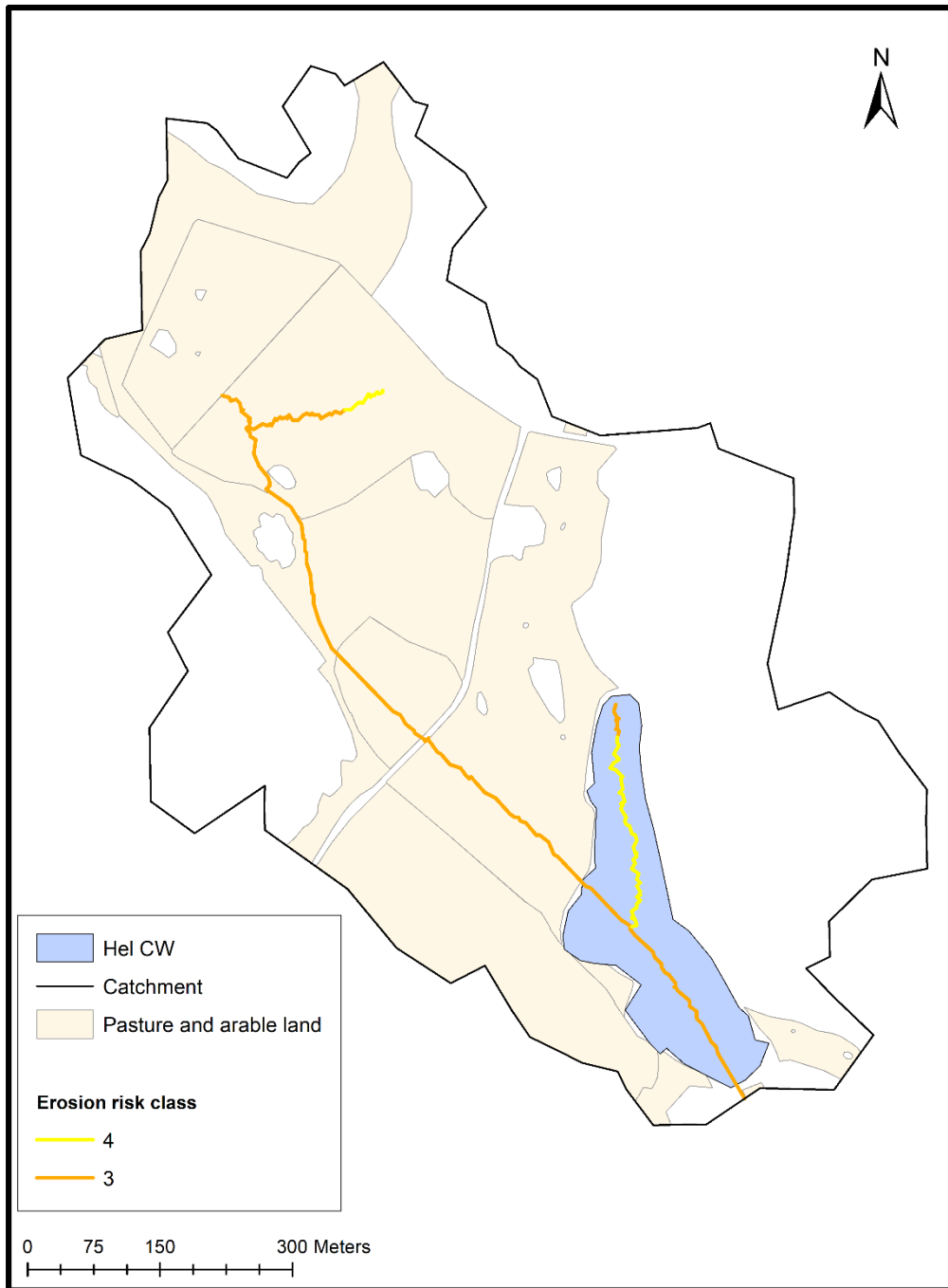


Figure 27. A map of Hel and its catchment area. Beige markings display pasture and arable land areas. Erosion risk classes vary from 3 to 4 within the catchment, where risk class 3 dominates.

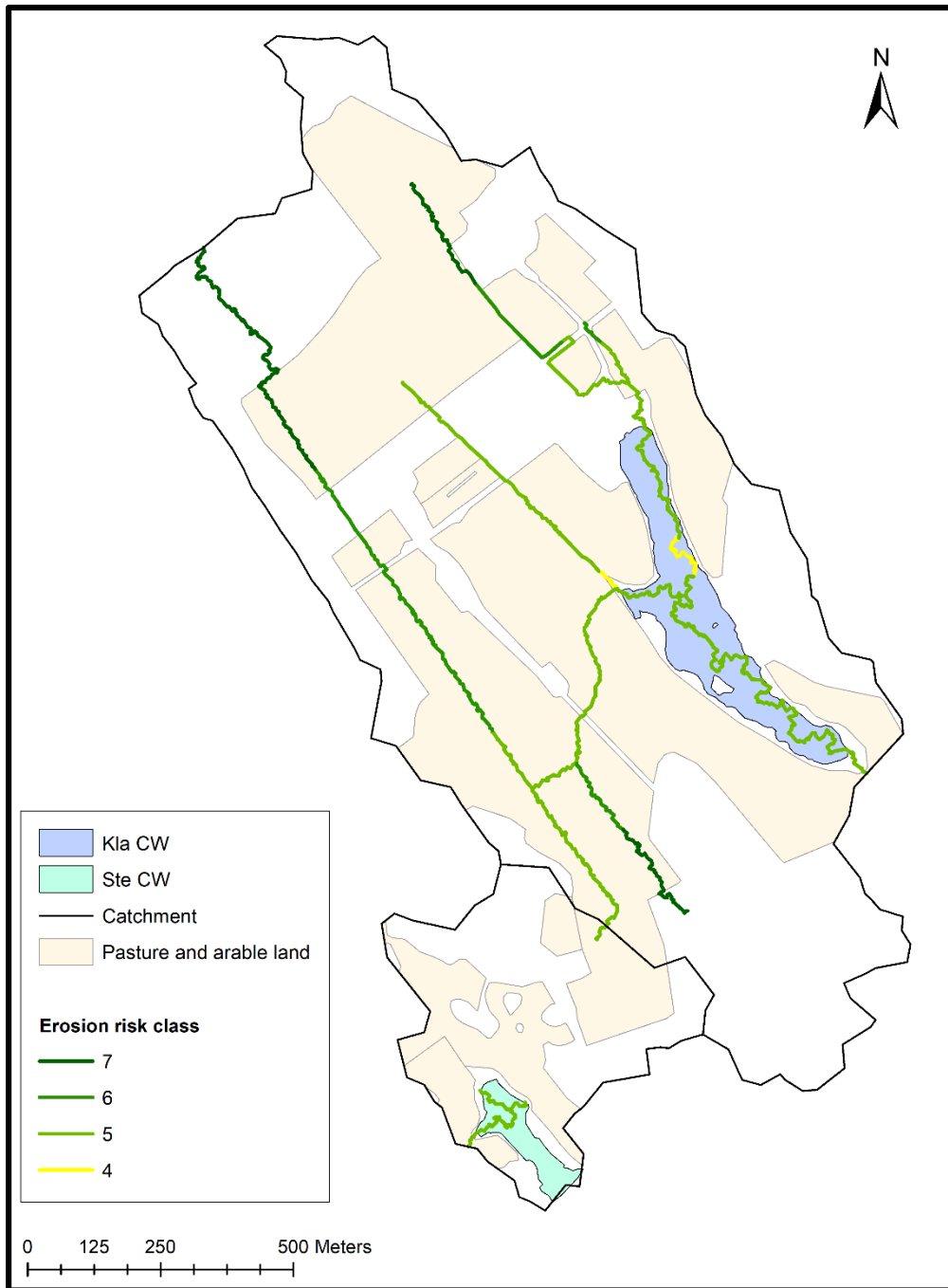
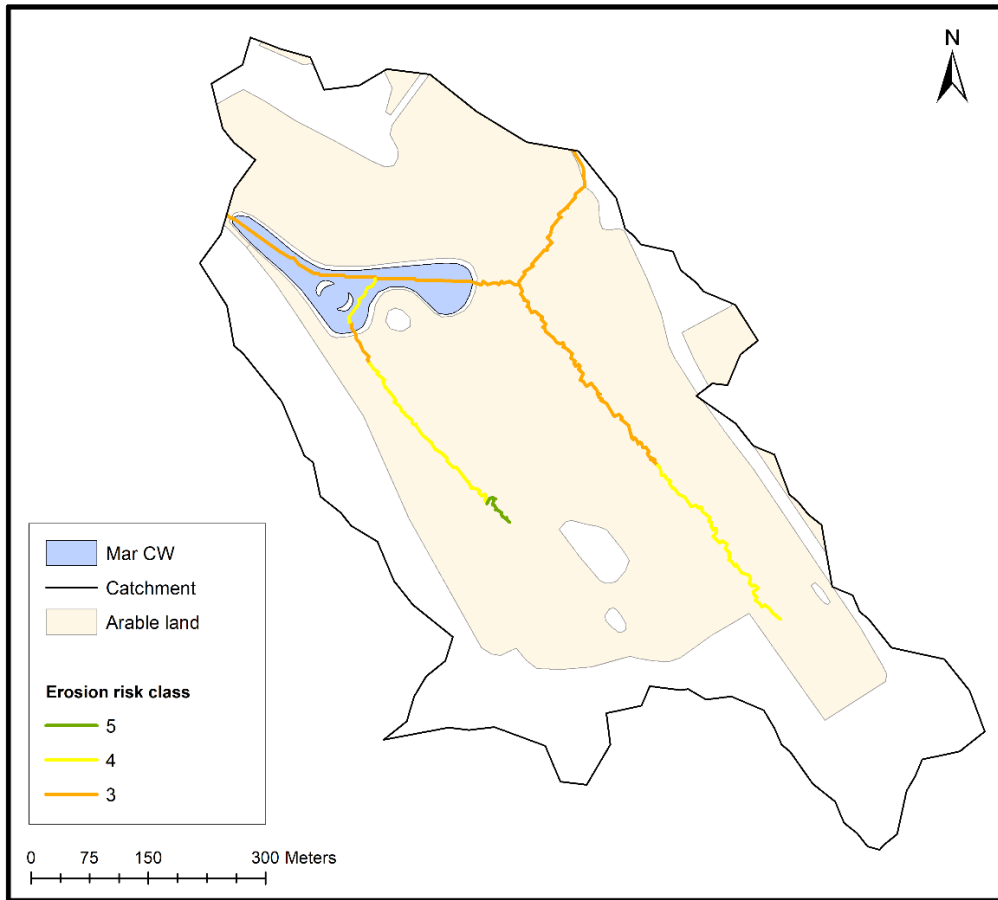


Figure 28. A map of Kla and Ste, and their corresponding catchment areas. Beige markings display pasture and arable land areas. Erosion risk classes vary from 4 to 7 within the catchments, where risk class 7 implies the lowest expected particle load. The dominating erosion risk class closest to the CWs is class 5.



*Figure 29. A map of Mar and its catchment area. Beige markings display arable land areas. Erosion risk classes vary from 3 to 5 within the catchment, where risk class 3 dominates.*

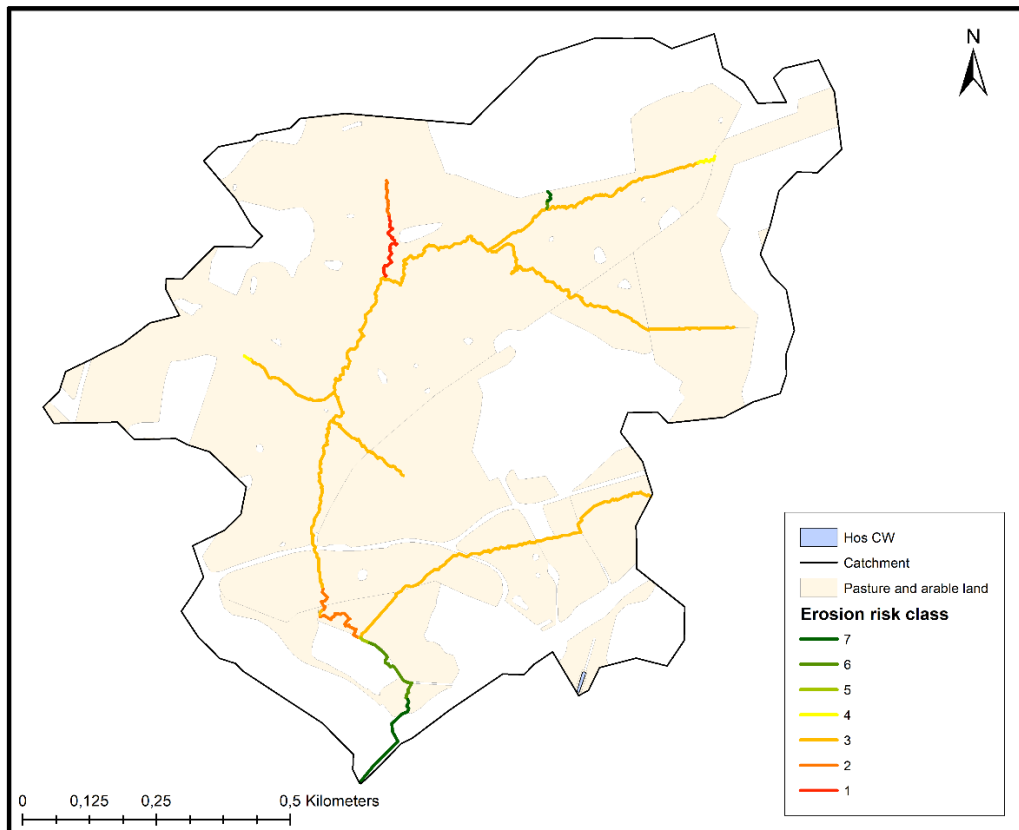
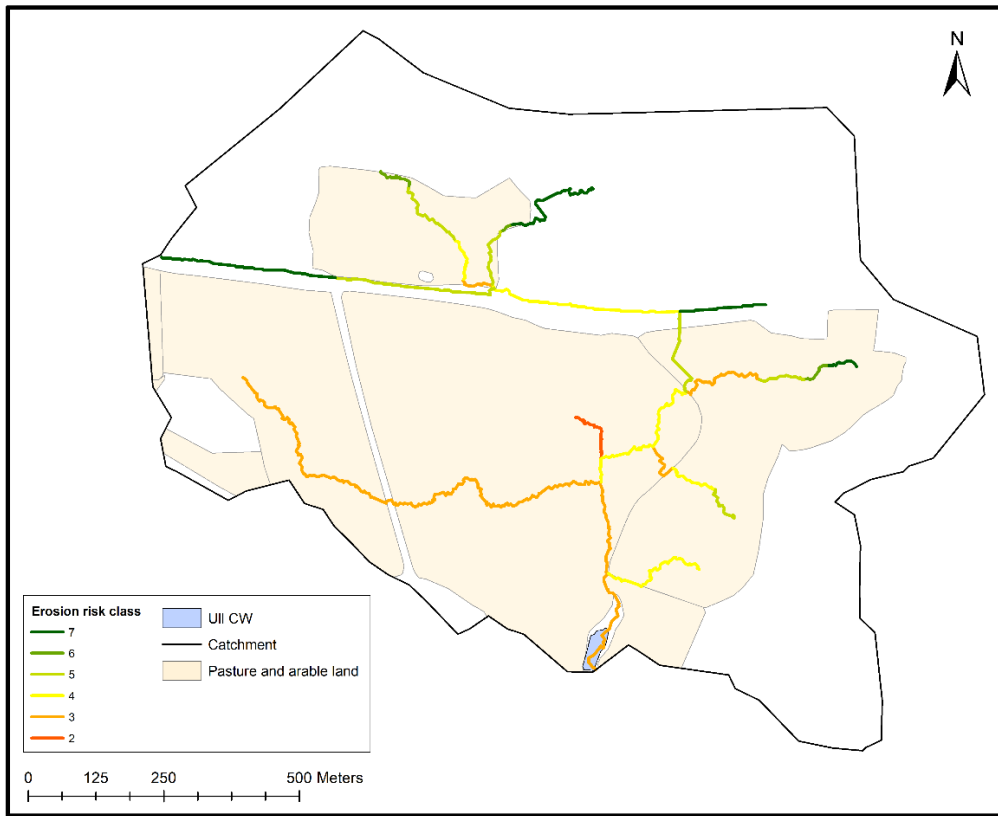
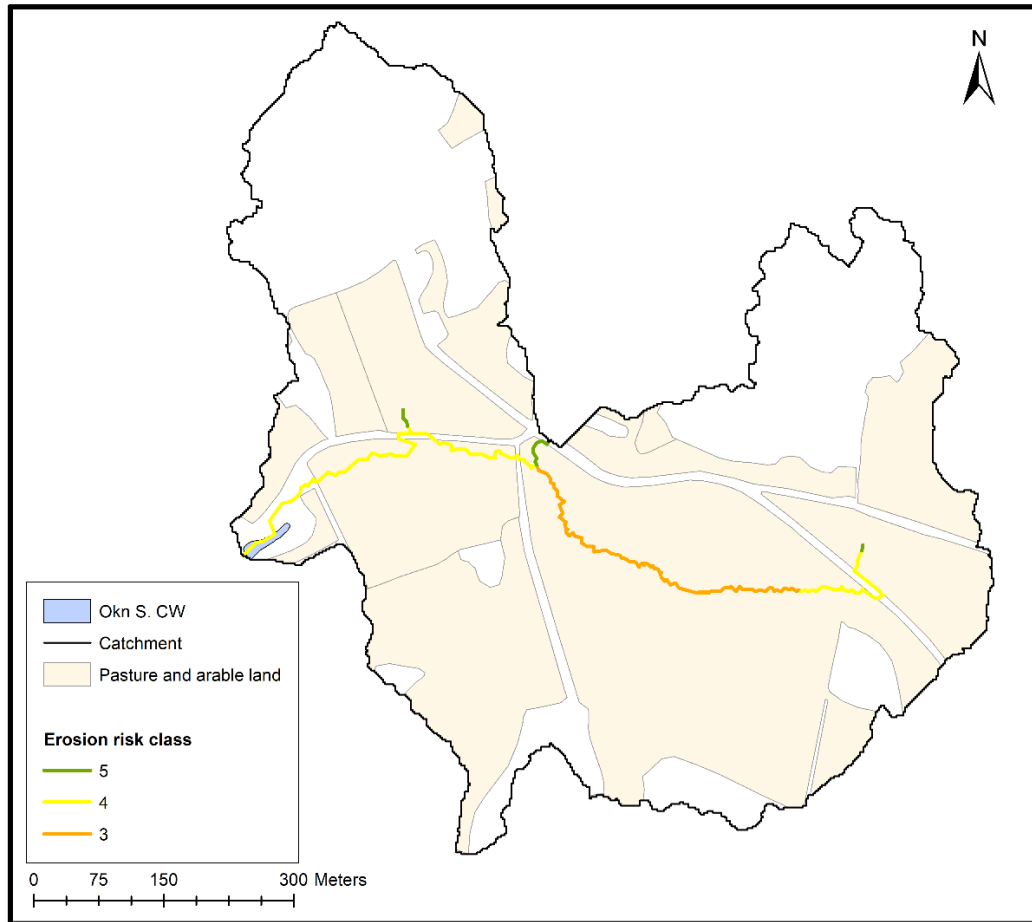


Figure 30. A map of Hos and its catchment area. Beige markings display pasture and arable land areas. Erosion risk classes vary from 1 to 7 within the catchment, where risk class 3 dominates.



*Figure 31. A map of Ull and its catchment area. Beige markings display pasture and arable land areas. Erosion risk classes vary from 2 to 7 within the catchment, where risk class 3 dominates.*



*Figure 32. A map of Okn S and its catchment area. Beige markings display pasture and arable land areas. Erosion risk classes vary from 3 to 5 within the catchment, where risk class 4 dominates.*

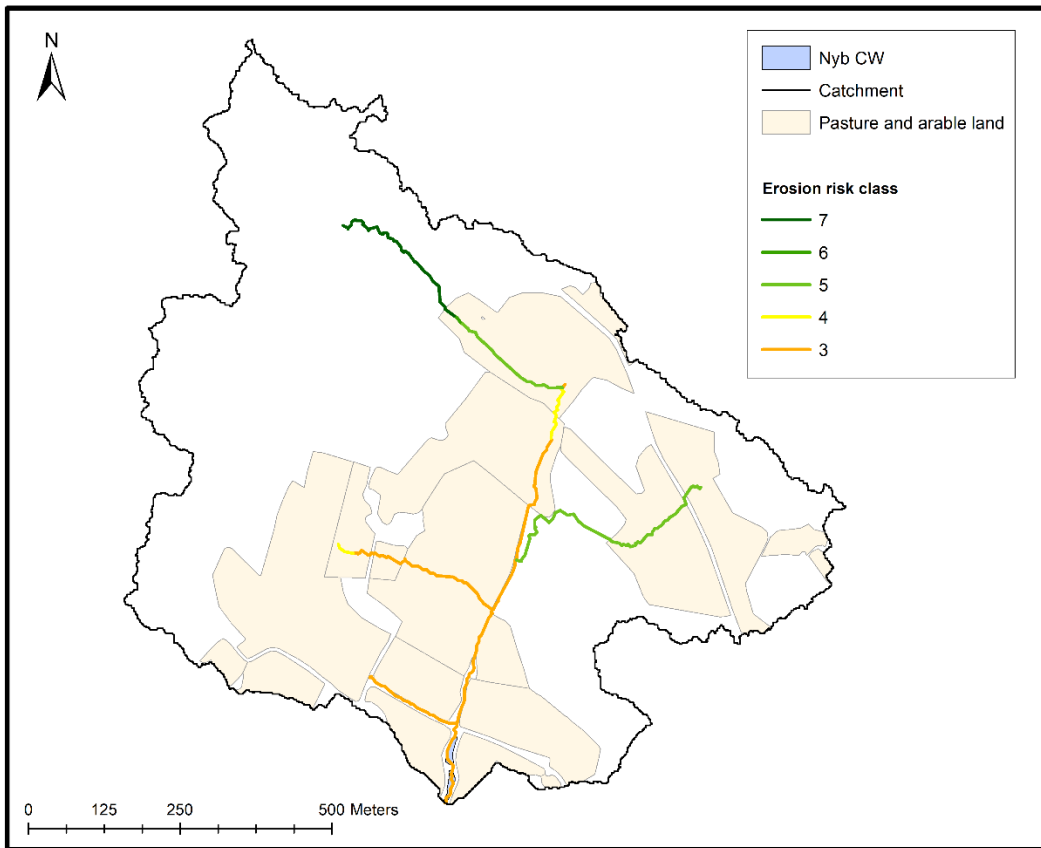


*Figure 33. A map of Nyb and its catchment area. Beige markings display pasture and arable land areas. Erosion risk classes vary from 3 to 7 within the catchment, where risk class 3 dominates.*